



Reviews of Geophysics

REVIEW ARTICLE

10.1002/2014RG000465

Key Points:

- Geophysics as a tool for imaging of critical zone processes
- Can image deep critical zone where direct measurements are limited
- Examples of recent successes and opportunities for the future

Correspondence to:

A. D. Parsekian,
aparseki@uwyo.edu

Citation:

Parsekian, A. D., K. Singha, B. J. Minsley, W. S. Holbrook, and L. Slater (2015), Multiscale geophysical imaging of the critical zone, *Rev. Geophys.*, 53, doi:10.1002/2014RG000465.

Received 27 JUN 2014

Accepted 10 DEC 2014

Accepted article online 13 DEC 2014

Multiscale geophysical imaging of the critical zone

A. D. Parsekian¹, K. Singha², B. J. Minsley³, W. S. Holbrook¹, and L. Slater⁴

¹Department of Geology and Geophysics, University of Wyoming, Laramie, Wyoming, USA, ²Department of Geology and Geological Engineering, Colorado School of Mines, Golden, Colorado, USA, ³U.S. Geological Survey, Denver, Colorado, USA, ⁴Department of Earth and Environmental Science, Rutgers, The State University of New Jersey, Newark, New Jersey, USA

Abstract Details of Earth's shallow subsurface—a key component of the critical zone (CZ)—are largely obscured because making direct observations with sufficient density to capture natural characteristic spatial variability in physical properties is difficult. Yet this inaccessible region of the CZ is fundamental to processes that support ecosystems, society, and the environment. Geophysical methods provide a means for remotely examining CZ form and function over length scales that span centimeters to kilometers. Here we present a review highlighting the application of geophysical methods to CZ science research questions. In particular, we consider the application of geophysical methods to map the geometry of structural features such as regolith thickness, lithological boundaries, permafrost extent, snow thickness, or shallow root zones. Combined with knowledge of structure, we discuss how geophysical observations are used to understand CZ processes. Fluxes between snow, surface water, and groundwater affect weathering, groundwater resources, and chemical and nutrient exports to rivers. The exchange of gas between soil and the atmosphere have been studied using geophysical methods in wetland areas. Indirect geophysical methods are a natural and necessary complement to direct observations obtained by drilling or field mapping. Direct measurements should be used to calibrate geophysical estimates, which can then be used to extrapolate interpretations over larger areas or to monitor changing processes over time. Advances in geophysical instrumentation and computational approaches for integrating different types of data have great potential to fill gaps in our understanding of the shallow subsurface portion of the CZ and should be integrated where possible in future CZ research.

1. Introduction

The “critical zone” (CZ) is Earth's breathing skin: a life-supporting epidermis that reaches from the top of vegetation down through soil, weathered rock, and fractured bedrock. The CZ transforms intact bedrock into regolith, soil, sediments, and ultimately into solutes through physical, geochemical, hydrological, and biological processes that occur from the top of the subaerial biological zone to the base of the groundwater zone. The rates at which those processes occur, the complex interactions among them, and their responses to ongoing natural and anthropogenic changes are topics of intensely accelerating research spanning an array of scientific disciplines. The recent establishment of a group of Critical Zone Observatories (CZOs) in the U.S., and a parallel network of global sites, spotlights the importance assigned by the global Earth science community to understanding CZ processes.

CZ research addresses issues of fundamental relevance to the ecological services that human societies depend on, including nutrient cycles, erosion and landscape evolution, and water supply and quality. For example, how fast does bedrock weather into regolith and soil, and what controls that rate? Where is water stored in the CZ, and how does CZ structure affect the exchange of water between surface and subsurface reservoirs? What role does the deep CZ play in supporting ecosystems? How thick is the regolith, and how do climate, mechanical failure, chemical weathering, and biologically mediated processes regulate that thickness? And how will CZ structure and function respond to ongoing global change?

Addressing such questions requires synoptic research that spans the full depth range of the CZ, from treetops to the base of fractured bedrock. While the upper part of the CZ—the vegetation, soil, and surface water—is readily accessible [e.g., *Jin and Brantley*, 2011; *Takagi and Lin*, 2011; *Johnson et al.*, 2012], the deeper reaches, where many processes occur, are often difficult to access. The thickness of the CZ varies from millimeters or centimeters (in bedrock outcrops) to many tens of meters (in heavily weathered terrains), but it

is seldom thin enough to sample completely with shovels, soil pits, and trenches. Drilling and augering are often employed to measure deep CZ properties and processes, but they have limitations: augering, while inexpensive, is limited to the depth of refusal, invasive, and typically limited to a few narrow, widely spaced holes. Drilling adds expense to that list—in the limited locations where it is possible to use the heavy drilling equipment needed to install deep wells. Lateral variability of lithologic, sedimentary, and hydrologic units—a common and important characteristic of the CZ—cannot be sufficiently mapped with these direct sampling methods. To study the deep CZ, geophysical techniques that can remotely sense changes or contrasts in the structure and physical properties of this otherwise inaccessible region may be deployed.

Fortunately, the recognition of the need to study CZ processes has been paralleled by important advancements in near-surface geophysical instrumentation and methodology. Over recent decades, the ability to acquire data over larger areas in more dimensions (including time) has greatly improved, while geophysical instruments have become smaller, lighter, and cheaper. As a result, it is now possible for small teams of scientists, working over a reasonable field campaign, to characterize the shallow subsurface over vertical scales from centimeters to hundreds of meters and at lateral scales from meters to kilometers. New algorithms and vastly improved computational power enable geophysical imaging with unprecedented resolution and improved understanding of uncertainties. Preliminary (but reliable) results can be produced for many methods in a matter of minutes to hours, enabling flexible field surveys in which data acquisition strategies can adapt to structural information as it is revealed. Finally, many geophysical methods are well suited to time-lapse measurements, allowing the study of processes over varying temporal (as well as spatial) scales [e.g., *Johnson et al.*, 2012].

All geophysical methods indirectly measure physical property distributions within the subsurface. Ground-penetrating radar (GPR) uses high-frequency electromagnetic waves that are sensitive to the dielectric permittivity of an Earth material; electrical resistivity tomography (ERT) uses a low-frequency electrical field to determine the electrical resistivity structure of the subsurface; seismic refraction uses elastic waves that reveal seismic velocity; and so forth. Data are typically acquired on or above the Earth's surface, but unlike most remote sensing techniques, geophysical data contain information about variability in subsurface properties. The depth of investigation and resolution depends not only on the physics of the method but also on the distribution of subsurface properties. In general, the various geophysical methods can provide information about depths from meters to tens or hundreds of meters, spanning the full extent of the below-ground CZ. By combining several geophysical methods, we can produce representations of CZ structure and processes that span the full range of relevant scales. These process representations may be then linked to geochemical, hydrological, and ecological data.

At the outset of the development of the CZO network, geophysical methods were recognized as a key tool for subsurface characterization, with the understanding that new tools might need to be developed in the future [*Brantley et al.*, 2006]. In this review we summarize the thrust of near-surface geophysics research most relevant to imaging the CZ, including examples of recent applications of these methods to CZ problems. We also identify the research challenges and present a vision for future application of geophysics to CZ research. We indicate how geophysical measurements can be advantageous for imaging CZ properties and processes, in particular for investigations of the deep CZ; present examples where geophysical methods have contributed to better understanding of CZ science objectives; and identify the scientific challenges that are currently faced within the field of geophysical applications to CZ science. A central theme of our paper is to show that discoveries within the deep CZ may be accelerated through application of geophysical methods over a range of scales in time and space.

2. Background on Geophysical Measurements

Due to the range of physical properties being explored and the diversity of instrumentation available for CZ studies, a brief overview of geophysical techniques is included below. For a more comprehensive technical review of the theoretical and procedural underpinnings of geophysical methods, the reader is referred to several excellent existing reviews referenced in each subsection. Readers who are already familiar with near-surface geophysics measurement methods may wish to skip to section 3.

2.1. Seismic Methods

Seismic methods exploit the propagation of elastic energy in the subsurface and are divided into reflection, refraction, and surface wave methods, depending on the principal wave types considered in each method:

reflected energy from sharp boundaries (velocity or density contrasts), refracted compressional (P waves with velocity V_p) or shear (S waves with velocity V_s) waves that bend through velocity gradients, and boundary waves that propagate along the surface ("ground roll"). All three methods involve recording the wavefield on geophones. Reflection and refraction seismic methods rely on the creation of seismic waves by active sources (sledgehammer, explosives, weight drops, and vibrators), while surface waves can be sourced either actively [Park *et al.*, 1999] or passively [Louie, 2001]. Reflection methods, extensively applied in the near surface (see review by Steeples [2005]), are often difficult to implement in the upper 50 m due to strong lateral and vertical variations in seismic velocity. Near-surface refraction and reflection methods have been reviewed by Rabbel [2010]. V_s provides a useful complement to V_p , as it responds differently to fluid saturation and fracture geometry [e.g., O'Connell and Budiansky, 1974; Pride, 2005]. Subsurface shear wave velocities can be deduced from either tomography of shear body waves (S waves) or by analysis of surface waves (Rayleigh or Love waves), which propagate at a large fraction of the shear velocity. Shear waves can be difficult to generate and detect in typical refraction work and usually require horizontal-component geophones and specialized sources [e.g., Grelle and Guadagno, 2009]. The most common way to estimate shear wave velocity in the critical zone is multichannel analysis of surface waves (MASWs), a technique that uses Rayleigh wave dispersion curves to derive (typically) one-dimensional models of V_s beneath a short array [Xia *et al.*, 1999; Socco and Strobbia, 2004].

2.2. Ground-Penetrating Radar

Ground-penetrating radar (GPR) is similar to seismics in that it is a wave-based geophysical method but uses the timed transmission and reflection of electromagnetic waves (10–2000 MHz) in place of seismic energy. Typically, GPR utilizes a single source-receiver antenna pair. Geometric information about the subsurface is obtained by traversing the target area with the antennas along survey profiles. This measurement is completely noninvasive as the antennas only slide across the surface of the Earth. Dielectric permittivity is the physical property that primarily governs electromagnetic (EM) wave velocity at GPR frequencies, which depends on water content due to the strong permittivity contrast between water (≈ 80) and air (≈ 1). To acquire velocity depth profiles that may be used to infer physical and material properties, it is typical to use multiple-offset measurements where the source and receiver are spread apart from a center point, to use the depth to a known reflector to convert measured traveltime and distance to velocity or to estimate velocity from diffractions produced by objects such as boulders or roots. The review by Neal [2004] and the textbook edited by Jol [2008] provide comprehensive information about the GPR method.

2.3. Electromagnetics

Active source electromagnetic (EM) methods respond to subsurface electrical conductivity. EM methods operate at lower frequencies than GPR and therefore rely on the physics of diffusion rather than wave propagation, allowing for much greater depth of penetration but with lower spatial resolution. EM measurements are made using loops or coils of wire and do not require direct contact with the Earth, allowing for rapid acquisition from airborne or towed platforms. Time-varying currents in a transmitter loop or coil induce EM fields in the subsurface that interact with geologic materials causing an electric current which in turn results in a secondary EM field that is detected in a receiver coil and contains information about the subsurface electrical properties. Instrumentation may be hand carried, towed behind a vehicle, deployed using wire loops or coils laid on the ground surface, or slung beneath an aircraft. Ward and Hohmann [1988] provide extensive additional details on EM geophysics, and Siemon *et al.* [2009] review airborne electromagnetic methods for large-scale mapping.

2.4. Nuclear Magnetic Resonance

Nuclear magnetic resonance (NMR) is unique among geophysical methods in that the measurement is directly sensitive to water. NMR uses electromagnetic fields to excite the state of hydrogen protons in water molecules within a background magnetic field and then detects the signal from those protons as they return from their perturbed state. Varieties of NMR instruments may utilize large wire loops on the Earth surface and the Earth's magnetic field or downhole logging tools with wire coils and permanent magnets. Please refer to Hertrich [2008] for additional details on the NMR method.

2.5. Electrical Resistivity Methods

Electrical resistivity tomography (ERT) is an active source geophysical method that uses a low-frequency electrical current that is galvanically injected into the ground between two electrodes and measures the difference in voltage between two or more different electrodes. This is a minimally invasive method because it requires placing electrodes a few centimeters into the ground to create electrical contact. This pattern is repeated through many combinations of transmitting and receiving electrodes along a line or grid, and the result is a cross section or volume distribution of electrically resistive or conductive regions in the subsurface. Charge storage in the Earth, typically associated with grain-fluid interface properties, can also be measured through the induced polarization (IP) method, both in the time domain or frequency domain. *Binley and Kemna [2005]* and *Zonge et al. [2005]* provide comprehensive descriptions of galvanic electrical geophysics.

2.6. Self-Potential Method

The self-potential method is a passive geophysical technique that is sensitive to active processes such as fluid flow, diffusion, and electrochemical transport and redox zonation. The result of these subsurface source mechanisms is potential voltage field (self potentials) that can be measured on the Earth's surface using a standard voltmeter and nonpolarizing electrodes. Analysis of the spatial distribution of self potentials can be used to make inferences about subsurface processes and can be highly complementary to other geophysical methods. *Revil and Jardani [2013]* provide a comprehensive review of the self-potential method.

2.7. Gravity Field

Passive gravity observations can provide key constraints on structural features such as basin thickness and fault geometry over a range of scales. Satellite-based gravity data (such as from Gravity Recovery and Climate Experiment (GRACE) [*Rodell et al., 2007*]) provide continental-scale information about geological structure and changes in hydrologic storage. Airborne gravity data provide important basin-scale information about geologic structure and faulting, while at the site scale, ground-based observations are used to delineate local changes in sediment or rock type. Microgravity measurements using accurate ground-based gravimeters have been used to monitor changes in subsurface water storage. Recent advances in airborne and ground-based gravity gradiometry instrumentation allow for the measurement of the full gravity tensor, rather than just the traditionally measured vertical component, promising improved capabilities to resolve subsurface structures. See *Nabighian et al. [2005]* for a review of gravity methods.

2.8. Distributed Temperature Sensing

Fiber optic-distributed temperature sensing (FO-DTS) exploits measurable changes in the optical properties along fiber-optic cables that result from temperature and strain variations. A laser pulse transmitted down the cable is affected by the changes in the glass fiber, and light backscattered from microscopic imperfections in the glass is detected at a sensor. The frequency shifts of this applied pulse are correlated to temperature, thus yielding a temperature measurement along the cable on the order of every meter. Please refer to *Selker et al. [2006]* for additional details on the FO-DTS measurement.

The following three other relevant topics are also important for brief discussion, beyond the methods detailed above.

2.9. Forward Modeling of Geophysical Data

Given that the underlying physics that each geophysical method is based on are well understood, it is possible to create forward models, or synthetic data sets, of geophysical measurements. There are two common examples of how forward modeling may be useful: for prediction and for interpretation. In terms of prediction, several geophysical methods (e.g., transient electromagnetic and ERT) have depth sensitivity or resolution that is determined by the physical properties of the subsurface at the study site. Therefore, forward modeling the data based on some general expectations of the subsurface target may provide useful information to guide survey design. A second reason that forward modeling may be useful is to guide interpretation of unusual targets. For example, if an unusual feature was observed in GPR data, it would be possible to model possible target geometries to explain what is seen in the field data. In some cases, forward models may be available from the authors of inversion routines [e.g., *Loke and Barker, 1996; Müller-Petke and Yaramanci, 2010*], while in other cases they may be independent [e.g., *Irving and Knight, 2006*].

2.10. Geophysical Data Inversion

Geophysical inversion is the mathematical process of constructing models of a physical property in the subsurface based on measured data and any a priori information about the subsurface that may exist. The basics of geophysical inversion can be found in many texts, including *Menke* [1989], *Tarantola* [2005], *Scales et al.* [2001], and *Aster et al.* [2005]. Because geophysical data are inherently ambiguous and uncertain, it is often advantageous to combine multiple types of measurements that have complementary sensitivities to the subsurface properties of interest. Joint inversion methods have emerged as a quantitative approach to integrate data from multiple geophysical methods or nongeophysical data (e.g., hydrogeologic) to create better constrained models [*Doetsch et al.*, 2010; *Irving and Singha*, 2010; *Pollock and Cirpka*, 2012].

2.11. Physical Property Relationships

Observed geophysical properties (e.g., resistivity, seismic velocity, and dielectric permittivity) are generally not equivalent to the material properties required by geologists or hydrologists (e.g., lithology, permeability, moisture content, and geochemical concentrations). Consequently, a rock physics relationship is used to relate the measured geophysical parameter to the material property of interest. While some joint inversion techniques circumvent the use of rock physics relations, we more commonly build relationships at the lab or field scale and apply them to the geophysical data or inversion results. Theoretical relations have only been proven for simple materials, and empirical relations are usually site specific. Application of rock physics relationships to inverted geophysical models is problematic due to nonuniqueness and variable sensitivity (see *Day-Lewis et al.* [2005] for an overview). For a review on rock physics methods, see *Mavko et al.* [1998] and *Lesmes and Friedman* [2005].

3. Geophysical Characterization and Critical Zone Process Observation Examples

Next, we highlight how geophysical measurements are able to image parameters related to CZ processes such as weathering, hydrology, and biogeoscience. Selected examples from the recent literature are provided to illustrate the unique information content of geophysics. We consider the scale of the observations, the physical relationships employed, and the significance of the data with respect to questions pertaining to CZ processes.

3.1. Regolith and Weathering

Weathering processes are at the heart of understanding the critical zone. The CZ largely consists of weathered regolith and the flora and fauna it sustains, yet fundamental questions about the controls on regolith generation remain unanswered. Recent hypotheses on regolith generation propose key roles for topographic stresses [*Slim et al.*, 2014], reactive transport and reaction kinetics [*Fletcher and Brantley*, 2010], chemical disequilibrium above the water table [*Rempe and Dietrich*, 2014], tectonic fracturing [*Clarke and Burbank*, 2011], and north versus south aspect [*Anderson et al.*, 2013]. These and other hypotheses make predictions about how regolith thickness should vary with topography, weathering, aspect, and erosion, but critical hypothesis tests are largely lacking due to a paucity of regolith thickness measurements across landscapes. Geophysical data can uniquely fill this knowledge gap.

Each of the geophysical methods described in section 2 has a unique strength in imaging regolith and weathering processes, but recent research has shown that these methods are most powerful when combined together. *P* and *S* wave velocities from seismic refraction surveys provide a fundamental constraint on the thickness of regolith, since weathering always reduces seismic velocities, either through the creation of pore space (which is filled with either air or water and thus necessarily lower in velocity than the bedrock) or through the replacement of higher-velocity parent minerals, such as plagioclase, with lower velocity weathering products, such as clay minerals [e.g., *Olona et al.*, 2010].

Seismic refraction is especially useful in terrains underlain by crystalline rock, where all units can be interpreted as either bedrock or its weathered products. In such areas, rock physics models of seismic velocities can provide estimates of porosity that show broad agreement with those calculated from in situ samples [*Holbrook et al.*, 2014]. However, seismic refraction does a relatively poor job of identifying lithological boundaries in sedimentary units, due to both the intrinsic limits of resolution of refraction images and the overlap in velocity between sedimentary rocks with high initial porosity (such as alluvial deposits) and regolith. A combination of methods is most likely to lead to improved interpretations of subsurface structure and properties.

Befus et al. [2011] used seismic refraction tomography to image the weathered zone of two alpine catchments, 0.46 and 2.7 km² in size, and found differences in regolith thickness depending on north/south aspect. This study was designed to test a watershed-scale hypothesis that different catchments would have different weathering depth to bedrock. Other studies have estimated weathering depth by comparing surface wave and *P* wave refraction data [*Casto et al.*, 2009] or refraction, surface wave and ERT data. As shown in Figure 1, *Olona et al.* [2010] demonstrate that V_P (Figure 1a), V_S (Figure 1b), and resistivity (Figure 1c) surveys produce images with different areas of sensitivity, although they can be interpreted to reveal similar subsurface patterns. Most important is the interpretation of the portions of the three data sets that are coincident (Figure 1d) where the pattern of low velocity and resistivity as an indicator of the highest weathering class (and vice versa for the lowest weathering class) can be observed and confirmed using borehole data. Furthermore, resistivity investigations calibrated with geophysical logging and multiscale surface measurements have proven to be effective for estimating regolith depth in conjunction with mineralogy to explain a limitation to the processes of weathering bedrock into saprolite [*Braun et al.*, 2009]. We note that this is site specific; the relationship may be reversed under certain geologic conditions, and therefore, the resistivity measurement must be combined with either direct validation or another data set (e.g., seismic) for accurate interpretation.

Within the regolith, hydrologic processes are key drivers of weathering. Geophysical measurements may sense parameters related to weathering, and numerous recent studies show the potential for geophysical tools to improve subsurface characterization. For example, *McClymont et al.* [2011] combined seismic, ERT, and GPR data to estimate hydrologic flow paths in a moraine (Figure 2) over a 250 × 200 m area and to a depth of 60 m. In this example, areas of high resistivity (labeled "HR" in Figure 2) are inferred to be unsaturated zones at varying levels of weathering. In contrast, the low-resistivity zones (labeled "LR" in Figure 2) are identified as groundwater zones, either in the unconsolidated moraine or in underlying fractured bedrock. By including flow through bedrock fractures and through the moraine over the bedrock, they were able to develop a conceptual model using geophysical evidence of water movement from recharge at high elevations in the catchment to a lower elevation pond. In a related study, *McClymont et al.* [2012] use seismic and GPR data to define bedrock topography that underlies moraine and talus deposits of an alpine watershed and combine this information with time-lapse gravity data to better understand changes in water storage. Using combined seismic and electrical resistivity data sets, *Holbrook et al.* [2014] revealed variability in degree of weathering within the regolith. At the scale of hundreds to thousands of square kilometers, airborne electromagnetic (AEM) data provide opportunities to map regolith thickness and geomorphological features relevant to hydrological processes [*Worrall et al.*, 1999]. *Jørgensen et al.* [2012] combined AEM, seismic, and borehole data to reveal the configuration of faults and sedimentary structures in an area of 730 km². *Vrbancich and Fullagar* [2007] used AEM methods to map sediment thickness and bedrock topography in a shallow seawater environment. One-dimensional seismic MASW inversions along a transect have been used to produce 2-D estimates of V_s , used to estimate depth to bedrock in the critical zone [e.g., *Parker and Hawman*, 2012]. In all such cases, the primary value of the surveys is the definition of the large-scale geometry of the geological units and the development of conceptual models for hydrological processes. The limitation of such information is in the ambiguity of the geophysical relationship to physical properties and the possibility for misinterpretation. For example, the interpretation in Figure 2 implicitly assumes that variations in saturation primarily drive the resistivity variation, although resistivity is also strongly controlled by groundwater composition, grain size, and mineralogy.

3.2. Erosion and Sediment Transport

Physical weathering in the form of sediment transport in rivers and streams has implications for geomorphology as well as nutrient cycling. The challenge with measuring sediment transport comes from the wide spatial and temporal scales over which this process occurs. The advantages of geophysical measurements to support estimates of sediment transport by surface water lie largely in the implementation of sensor arrays in time-lapse mode. *Hsu et al.* [2011] observed that using time-lapse passive seismic measurements combined with information about river stage and discharge allowed for a mapping of transport of gravel over a river bottom. *Rickenmann et al.* [2012] use a combination of time-lapse seismic and direct automated sampling to calibrate passive seismic measurements to fluvial processes such as transported bed load mass, a methodology that has been deployed in several different stream and river environments [*Rickenmann et al.*, 2012, 2014; *Schmandt et al.*, 2013]. Passive seismic sensors have also been

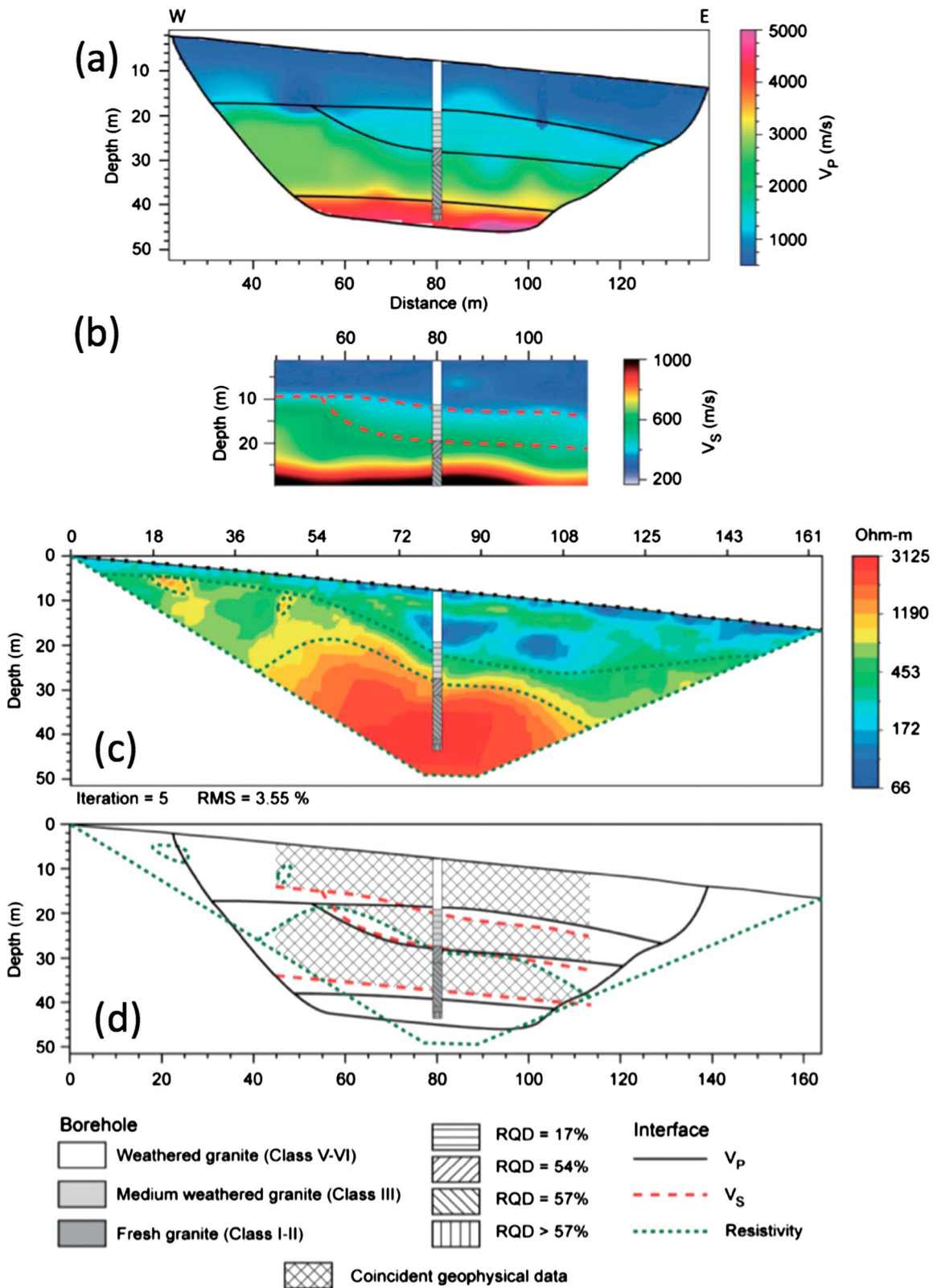


Figure 1. Weathering variations in a granitic massif. (a) V_P (b) V_S , and (c) resistivity geophysical models and interpreted interfaces with core log overlaid. (d) A joint comparison of interfaces from geophysical models shows where the three field measurements agree, largely in the high-sensitivity portion of the cross section. RQD indicates Rock Quality Designation, a measure of rock fracture in the rock. This demonstrates repeatable results and value of joint imaging (figure reprinted from Olona et al. [2010]).

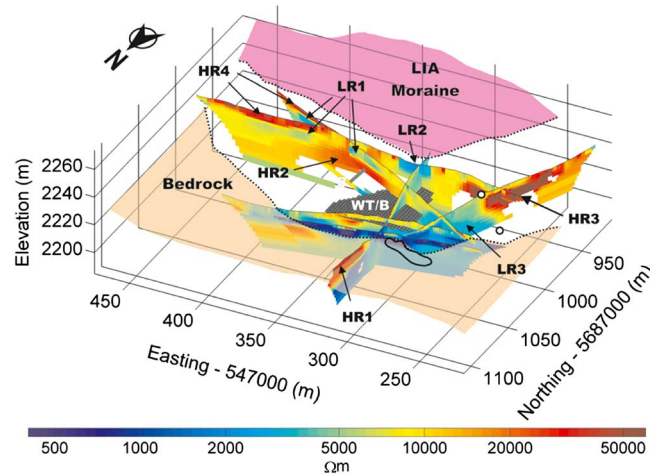


Figure 2. Six ERT tomograms viewed in 3-D space within a proglacial moraine. Gray mesh shows interpolated water table (WT) and bedrock (B) reflections. HR1-4 and LR1-3 indicate high- and low-resistivity anomalies, respectively. Circles define the location of two small groundwater springs (figure reprinted from *McClymont et al.* [2011]).

demonstrated to be effective at locating the spatial position of mass wasting events in mountain catchments where background seismic noise is low compared to the sediment transport signal [*Burtin et al.*, 2013]. The primary strength of such approaches is the potential to detect catchment-scale geomorphological events, including those that are invisible to remote sensing techniques. However, research is needed to fully understand event detection limits, resolution in relation to spacing of seismic sensors and accuracy of event location [*Burtin et al.*, 2013].

3.3. Preferential Hydrologic Pathways

Water movement through preferential pathways in the subsurface—specifically:

How much? Where? and When?—is an open area of uncertainty in CZ hydrology. These questions are related to hypotheses, for example, that preferential pathways drive solute transport [e.g., *Wildenschild et al.*, 1994], impact biological activity [*Wang et al.*, 2013], and influence partitioning of water in the hydrologic budget [*Tetzlaff et al.*, 2014]. Geophysical tools have frequently been used to image subsurface preferential pathways that are important for determining where water moves and consequently control solute fluxes. These preferential pathways are usually defined by hydraulic conductivity heterogeneity, which geophysical measurements may be sensitive to, especially if time-lapse measurements are collected. For example, surface-based GPR surveys [e.g., *Grasmueck*, 1996; *Tsofilias et al.*, 2004] have been used to detect fractures by capitalizing on the contrast in dielectric permittivity between solid phase geologic materials and the fluid that fills the fractures. ERT has also been successfully used in fractured rock environments [e.g., *Hansen and Lane*, 1995; *Slater et al.*, 1997], and new inversion techniques have recently been investigated for ERT to map fracture zones more accurately by explicitly incorporating known fracture locations from wellbore logs [*Robinson et al.*, 2013]. Active source *S* wave tomography studies, often combined with *S* wave reflection imaging, have been used to image subsurface fault zones [*Catchings et al.*, 2014] and buried esker aquifers [*Pugin et al.*, 2009]. Preferential pathways in limestone have been imaged with GPR, leading to new understanding of how water moves through dissolution features and is stored in the aquifer over short (i.e., storm) and seasonal timescales [*Truss et al.*, 2007]. Self-potential observations have also been used to map preferential flow associated with buried channels [*Revil et al.*, 2005] and to advance understanding of the dynamic hydrologic behavior within collapse conduits in covered karst environments [*Bumpus and Kruse*, 2014]. Geophysical tools have also been shown to be effective at mapping preferential pathways in the unsaturated zone. Through experiments on synthetic macropores, *Moysey and Liu* [2012] suggest that flow through preferential pathways in soil can be detected using ERT if the resistivity of the soil matrix is sufficiently high that surface conduction can be ignored. During an investigation at a hillslope field site, *Cassiani et al.* [2009] were able to demonstrate using time-lapse ERT that direct infiltration into soil and bedrock at their study site is responsible for the majority of precipitation transport—important knowledge that can enable accurate modeling of hillslope hydrologic processes. In another hillslope study, *Leslie and Heinse* [2013] demonstrated the ability of ERT measurements to image soil pipes as preferential flow paths (Figure 3), thus providing an explanation for subsurface hillslope drainage processes. In this example after forest burning, the locations of soil pipes within ~0.35 m of the surface were imaged as high-resistivity anomalies (Figure 3), in most cases corresponding with directly observed excavated soil pipes. *Sassen et al.* [2009] used high-resolution GPR to reveal the function of roots as preferential flow paths guiding water deeper into the subsurface. In all cases, preferential flow paths can only be identified when the size of the pathway is large enough to generate a measurable anomaly in the geophysical signature at the selected

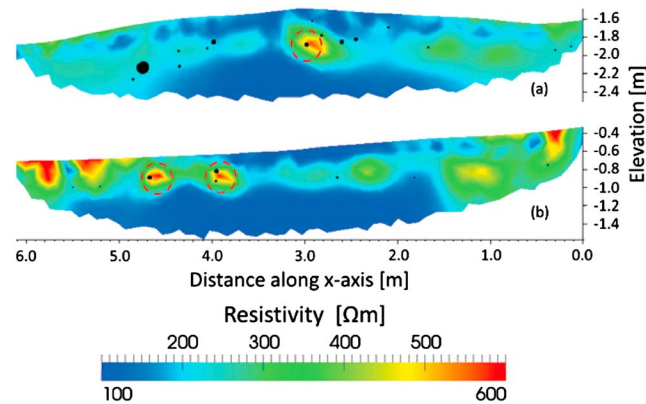


Figure 3. Resistivity tomograms of the root zone after a burn event: 2-D slices and measured soil pipe cross-section positions (black circles) from excavation with interpolated continuous soil pipes; red dashed circles highlight measured pipes that coincide with resistivity anomalies (figure reprinted from *Leslie and Heinse* [2013]).

preferential flow paths can overcome this limitation as transport is directly detected but may not be practical. Self-potential signals are unique in that flow is directly detected under the right conditions. *Wishart et al.* [2006, 2008] demonstrated how self-potential signals could be used to directly detect directions of flow in fractured bedrock and that such information could not be obtained from resistivity measurements.

3.4. Groundwater/Surface Water Interaction

Interaction of surface waters with surrounding aquifers provides ecosystem services [e.g., *Brunke and Gonser*, 1997; *Krause et al.*, 2011] such as thermal buffering, metal uptake, and denitrification. Open questions associated with groundwater-surface water exchange include the time-variable extent of the hyporheic zone and geologic controls on exchange processes [e.g., *Wroblecky et al.*, 1998]. One of the advantages of geophysical tools in these systems is that they can provide a more complete picture of the subsurface than can be achieved from in-stream measurements or piezometers alone, which is the standard way of characterizing processes occurring within aquifers surrounding streams. Geophysical methods can also help to address some limitations of reach-scale studies that estimate upstream behavior based on limited downstream observations in the surface stream.

Geophysical data, particularly ERT, have become commonly used to look at controls on exchange processes [e.g., *Ward et al.*, 2010; *Cardenas and Markowski*, 2011; *Toran et al.*, 2012]. ERT has been used to map the architecture and heterogeneity of subchannel sediments controlling exchange beneath streams [*Cardenas et al.*, 2004]. *Ward et al.* [2010] demonstrated the use of time-lapse ERT imaging coupled with electrically conductive solute tracers to image the hyporheic zone in two dimensions across a transect of a low-gradient stream. Geophysical measurements have also allowed scientists to directly map changes in hyporheic zone extent using tracer tests [e.g., *Ward et al.*, 2012], natural tracers from infiltration [*Coscia et al.*, 2011], or stage changes [*Johnson et al.*, 2012]. In general, most studies have explored stream systems on the tens of meters to kilometer scales, although larger-scale imaging is possible. For example, in transitional coastal environments, AEM data have been used to map saltwater intrusion at scale of over tens to hundreds of square kilometers to study processes where fresh and saline surface waters mix with groundwater [*Fitterman and Deszcz-Pan*, 1998; *Viezzoli et al.*, 2010]. Similar applications of AEM to inland environments revealed the presence of saline sediments in an aquifer system related to a paleo-Okavango Megafan [*Meier et al.*, 2014].

Slater et al. [2010] combined waterborne ERT/IP imaging with FO-DTS to investigate groundwater-surface water interaction along ~3 km reach of the Columbia River, Washington (Figure 4). The main outcome was to reveal exchange between the river and geologic contacts that outcrop into the river (Figure 4a). Induced polarization imaging was used to determine the formation thickness (Figure 4b, left) and help to infer zones where water could exchange. These methods successfully mapped variations in the thickness of the aquifer unit along the river corridor, which was shown to focus exchange of river water and groundwater and to control uranium transport (Figure 4b, right). *Mwakanyamale et al.* [2013] showed that FO-DTS data from the same portion of the

measurement scale. Consequently, detection of small-scale features that may exert a strong control on flow and transport will inevitably be limited to imaging over small spatial scales. Furthermore, the regularization constraints associated with inverse modeling, particularly with resistivity methods, may often smooth out fine-scale features and prevent their detection. Features identified in static geophysical surveys must be interpreted with caution as, for example, an electrically conductive feature does not necessarily equal a hydraulically conductive feature. Time-lapse monitoring of tracer transport in

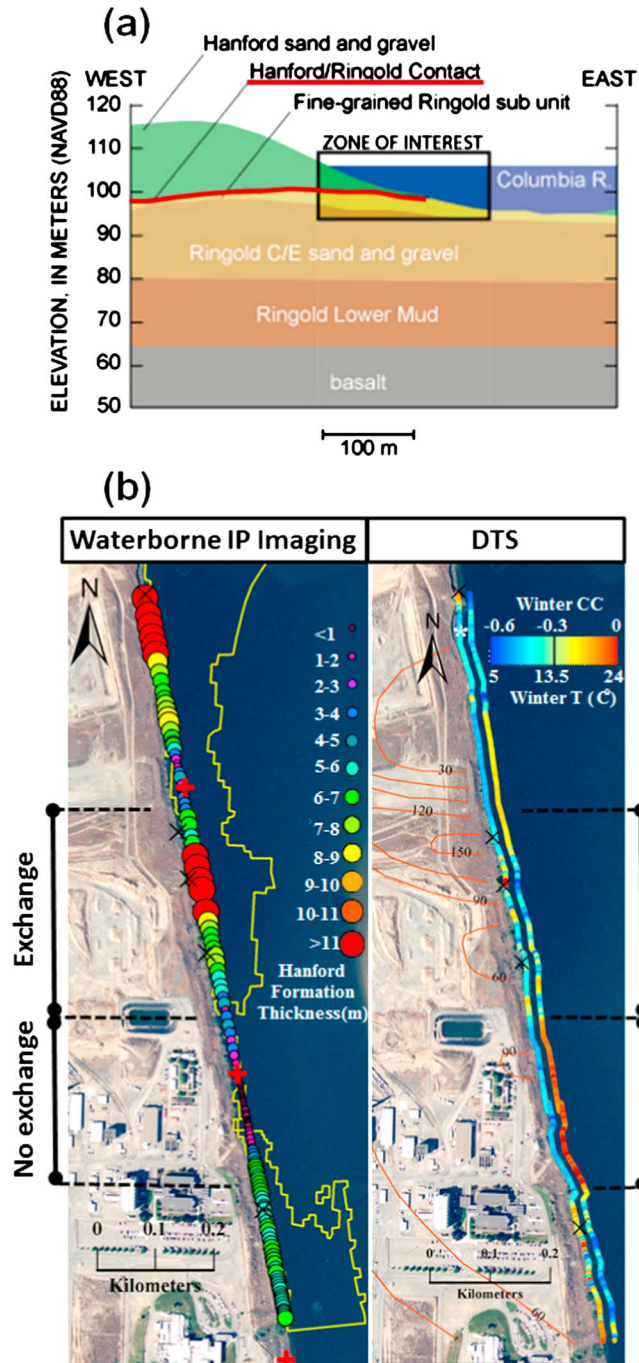


Figure 4. Integration of waterborne resistivity/induced polarization imaging with fiber optic-distributed temperature sensing (FO-DTS) along the Columbia River corridor adjacent to the U.S. Department of Energy Hanford 300 Area: (a) simplified geologic cross section of the site highlighting aquifer (Hanford) and semiconfining (Ringold) formations. The Hanford-Ringold contact limits vertical transport and directs groundwater toward the river. (b) Variations in Hanford formation thickness estimated from resistivity/IP imaging (left) compared with locations of focused exchange determined from FO-DTS during winter months when exchange locations are associated with high-temperature anomalies that show a negative correlation with river stage. Yellow box in the left image is estimated extent of Hanford outcrop on river bed from projections of borehole data inland. Orange contours in the right image are uranium contours in $\mu\text{g/L}$. Figure modified from Slater *et al.* [2010].

Columbia River site could reliably quantify exchange versus nonexchange zones. Johnson *et al.* [2012] revealed the inland extent of the surface water/groundwater interface resulting from variations in river stage using time series analysis of continuous time-lapse ERT data. The combined outcome of these geophysical measurements was a much improved understanding of the controls on groundwater/surface water interaction that can be used to improve conceptual and numerical models for contaminant transport at this site [Hammond and Lichtner, 2010].

Groundwater/surface water interaction is also important in the CZ of cold regions, where the existence of permafrost may serve as a hydrologic barrier that controls geochemical transport from the terrestrial environment to rivers and streams [Walvoord *et al.*, 2012]. Thaw through permafrost may result in a permeable hydraulic pathway that connects surface water and groundwater and has been identified as one mechanism that may drive the number and aerial extent of lakes [Yoshikawa and Hinzman, 2003; Roach *et al.*, 2011]. Minsley *et al.* [2012] gained insight into how permafrost and surface features relate to regional hydrologic systems using AEM data acquired over more than 300 km^2 in the Yukon Flats, Alaska (Figure 5). In the horizontal slices from the surface and 45 m depth (Figures 5a and 5b), it is possible to see cool colors indicative of frozen ground and the notable warm diagonal stripe in the northeast section that represents unfrozen ground. Similar information can be gleaned from the profile (Figure 5c) to visualize spatial variability in total permafrost thickness (black dashed line). These AEM data revealed extensive connections between lakes and rivers and deep aquifers below the frozen sediments that were

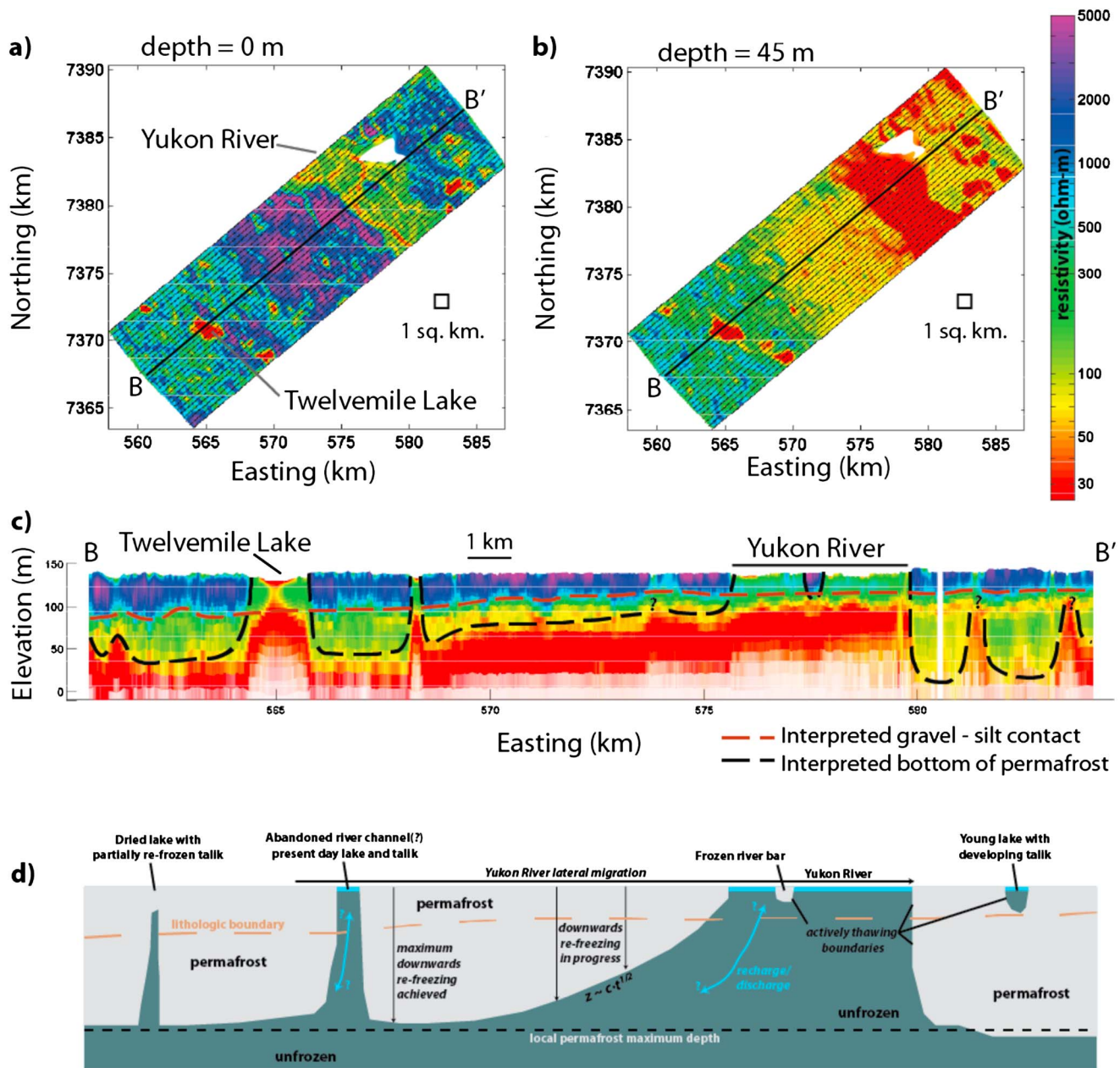


Figure 5. Spatial coverage of 300 km² portion of AEM survey in the Yukon Flats, Alaska. Map view slices through (a) the resistivity model at 45 m depth and (b) a cross section along a single ~25 km long profile B-B' show the detailed regional-scale hydrologic information that can be obtained to depths in excess of 100 m. (c) Resistivity data are used to infer extent of permafrost within both of these units (black dashed line) and therefore locations where the deep groundwater is linked to the surface. Conceptual process-based permafrost interpretation based on the resistivity cross section in Figure 5c. Permafrost is interpreted to be absent beneath the largest surface water features in the study area, most notably the Yukon River and Twelvemile Lake, whereas many smaller surface water features do not appear to fully penetrate the permafrost (figure reprinted from *Minsley et al.* [2012]).

previously unknown and enable interpretation of thaw processes (Figure 5d). Based on AEM results and Landsat-derived lake area change data, *Jepsen et al.* [2013] concluded that on a multidecadal timescale, shallow permafrost thaw linked to suprapermafrost flow in permeable aquifers is a more important driver for lake area change than thoroughgoing groundwater/surface water connections. At the even larger spatial scale of major river basins of North America and Eurasia, *Muskett and Romanovsky* [2009] use satellite-based gravity data (GRACE) to assess time-lapse water mass equivalent changes. Observed changes in groundwater storage are attributed to differences in permafrost extent in these basins and the development or expansion of throughgoing thaw zones that connect surface water and groundwater zones.

The benefits of using geophysical methods to investigate groundwater/surface water interaction therefore primarily relate to improving understanding of streambed/aquifer architecture and determining the location, timing, and spatial extent of exchange. The treatment of time-lapse geophysical data sets as a spatially expansive array providing proxy measures of pore fluid chemistry in the zone of interaction provides new opportunities to interrogate the relationship between external driving forces (river stage levels, recharge) and the result exchange. Extraction of quantitative hydrological data, e.g., on fluxes of groundwater or surface water across the groundwater/surface water interface, is unlikely using geophysical methods as defined in this review. However, time-lapse measurements of temperature profiles in the stream bed do provide an opportunity to constrain fluxes of groundwater into surface water [e.g., Keery *et al.*, 2007].

3.5. Watershed-Scale Hydrologic Processes

Watershed-scale groundwater model development requires information over larger areas than can be covered by typical ground-based geophysical surveys. For this reason, AEM is a natural complement to large-scale studies because of its ability to map the subsurface over large areas with dense spatial sampling, providing detailed information about the distribution of physical properties that control hydrologic processes at these scales. Recent efforts have aimed to directly integrate information derived from an AEM survey into groundwater models to improve model calibration and prediction accuracy and to quantify hydrologic prediction uncertainty [Refsgaard *et al.*, 2014; Seifert *et al.*, 2008].

Some AEM examples applied to large-scale hydrologic characterization include mapping buried valley aquifer systems in conjunction with seismic, resistivity, and borehole data [Jørgensen *et al.*, 2012; Oldenborger *et al.*, 2013]; imaging the geometry of surficial aquifer systems for parameterization of groundwater models [Abraham *et al.*, 2012]; and characterizing the spatial variability of floodplain sediments impacted by variable salinization and lateral recharge [Viezzoli *et al.*, 2009]. Over several thousand square kilometers in the southern Española Basin, aeromagnetic, gravity, and auxiliary geological and geophysical data were used to map basin sediments, bedrock geometry, and faults that provide important controls on the regional hydrogeologic framework [Grauch *et al.*, 2009].

In western Nebraska, AEM data were acquired in 2008 and 2009 in the areas surrounding the North Platte River and Lodgepole Creek, a tributary to the South Platte River, for the purpose of developing improved geological frameworks for groundwater models [Smith *et al.*, 2010; Abraham *et al.*, 2012] (Figure 6). The geometry of the high-resistivity alluvial sands and gravels that compose the surficial aquifer on top of the low-resistivity siltstone-confining unit (Figure 6a) is clearly imaged over most of the cross section to depths of approximately 80 m. This enabled the definition of a new “base-of-aquifer” boundary (Figure 5b, brown shading) that has considerably more detail than the older model input (Figure 5b, smooth black line). The AEM-derived base of aquifer geometry was used to parameterize groundwater models for the study area. Defining the geometry of the aquifer, including paleochannels and other small-scale features not identified from sparse borehole data, has significant impact on flow paths. Furthermore, an additional 458×10^9 L of potential additional water storage was identified (34% increase) based on estimated changes in the base of aquifer geometry.

These studies demonstrate that the primary benefits of watershed-scale applications of geophysical methods relate to the continuous imaging of geological structures that can be used to refine groundwater flow models that are often parameterized on sparse data points available from a limited number of boreholes. However, assigning hydraulic properties required to calibrate groundwater models using imaged geophysical properties is highly uncertain and should only be considered if independent constraints are available, e.g., petrophysical calibrations from measurements in boreholes or on representative samples in the laboratory. Even then, scaling issues, the limitations of petrophysical calibrations and complications of image regularization artifacts all discourage such an approach. Time-lapse monitoring of watershed-scale hydrological processes is currently very challenging compared to other scales but may become more common place in the future, e.g., with the deployment of geophysical sensors on drones.

3.6. Catchment-Scale Snow Processes, Distribution, and Water Equivalent

In the alpine CZ, snow is the main connection between atmospheric and terrestrial water and drives catchment-scale hydrology. Understanding snow depth, distribution, and snow water equivalent (SWE) across large areas on the scale of one or more watersheds is fundamental to understanding water availability

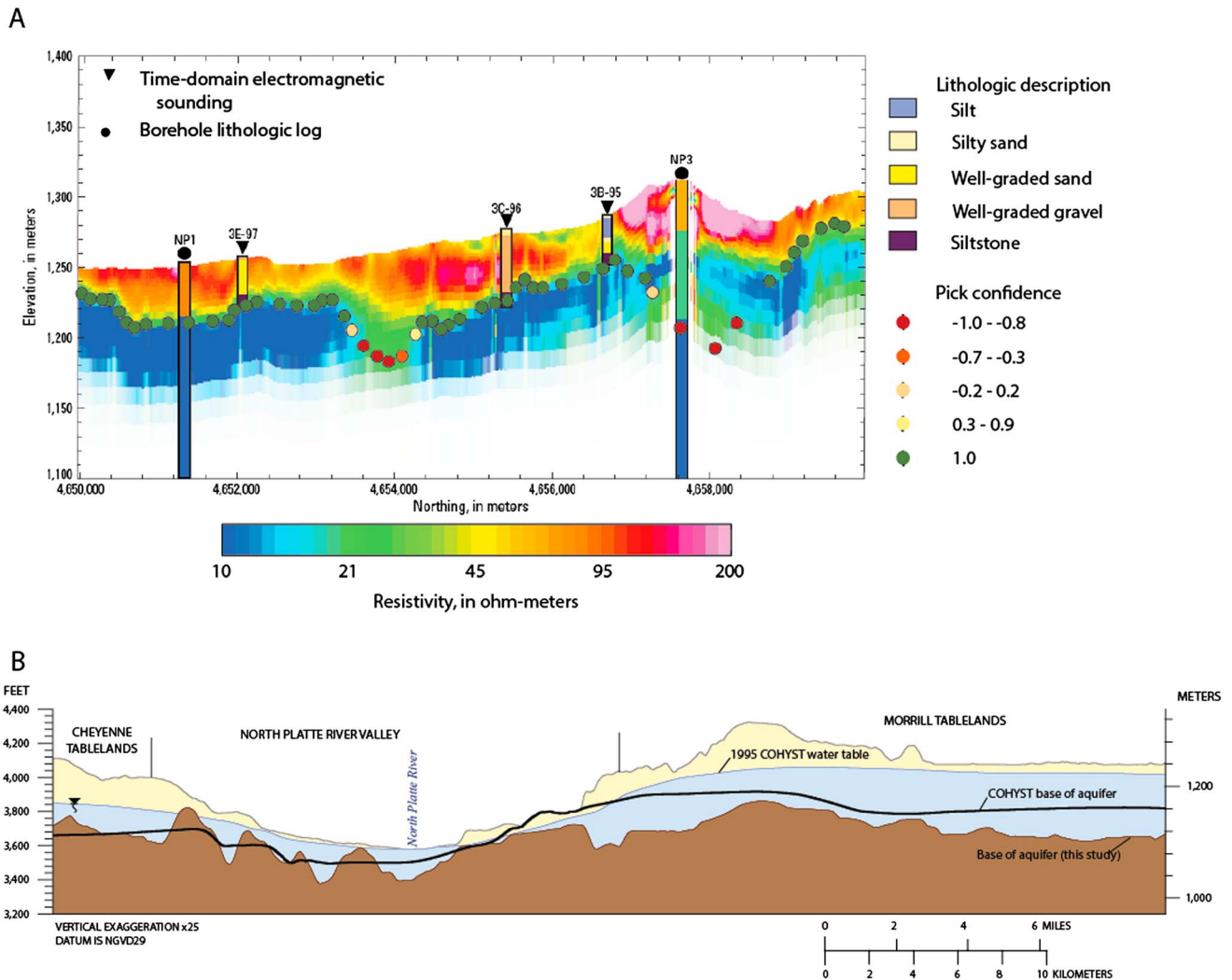


Figure 6. (a) Inverted resistivity section of part of helicopter electromagnetic flight line from the Nebraska study area. Lithologic data from nearby drilled wells are shown for comparison. (b) Interpreted cross section comparing data used by the hydrologic model between the 1995 COHYST (black line) and current data (brown shaded zone). Improvement is demonstrated by the increased level of detail in the brown base of aquifer interpretation. (figure reprinted from Abraham et al. [2012]).

for ecosystem function, river discharge, surface water/groundwater interactions, and weathering processes in these systems. GPR is an ideal geophysical tool for studying snow because the signal easily penetrates snow (a resistive material), the snow/ground interface has a strong contrast in physical properties that yields a reliable reflection, and data acquisition is fast. GPR is effective for traversing large areas to estimate snow depth [Marchand and Killingtveit, 2001] and SWE for dry snowpack [Jaedicke, 2003; Lundberg et al., 2006] using snow density relationships [Sand and Bruland, 1998]. More recently, techniques have been pioneered to extract SWE information about snowpacks with liquid phase water distributed among the solid phase ice/water matrix [Bradford et al., 2009; Sundström et al., 2013]. Such geophysical investigations have resulted in better understanding of the relationships between snow depth and slope aspect and snow depth and elevation [Marchand and Killingtveit, 2001].

3.7. Ecology and Biogeoscience of the Critical Zone

3.7.1. Root Zone Processes

In the context of the CZ, plant roots are the direct link between biological, hydrological, and geological components of the system, forming a dynamic, connected pathway between the geosphere and atmosphere. Roots are relevant to ecological models at various scales from the individual tree [e.g., Katul et al., 1997] to global atmospheric hydrology [Jackson et al., 2000]. In forest ecosystem process models,

tree roots compose a portion of forest biomass that must be estimated to study carbon balance [Running and Gower, 1991]. Models aiming to predict water movement, biomass, and carbon balance of the CZ must include parameterizations of roots. Geophysical measurements can improve model parameterizations related to roots because the measurements can be noninvasive (or nearly so) and spatially dense. By not destroying the target (i.e., digging up the roots manually), the system remains intact and time-lapse sampling becomes possible. Two geophysical methods have been applied to root investigations: GPR and ERT. Under ideal conditions, signal patterns in GPR data, known as diffractions, are useful for identifying the spatial location of roots greater than 0.005 m diameter within 0.15 m of the surface [Butnor *et al.*, 2001] and even estimating the root diameter [Barton and Montagu, 2004]. In an effort to quantify below-ground biomass, Yokota *et al.* [2011] used 3-D GPR acquisition to identify the location of roots surrounding a tree that was then excavated to verify the observed positions. Zenone *et al.* [2008] used both GPR and ERT for studying the shape and position of roots in a pine forest.

Despite what would appear to be a promising method, there are important limitations to the application of GPR for root investigations. The primary limitation is that diffraction patterns from overlying roots may mask signals from deeper roots; any interpreted GPR data indicating multiple depth levels of roots should be viewed with caution. A second important limitation is the fundamental resolution, related to antenna frequency, that limits the smallest diameter root that can reliably be detected [Hirano *et al.*, 2008]. Additionally, subsurface clutter such as stones and spacing between roots can lead to spurious interpretation.

Although the target resolution of ERT is typically unsuitable for studying individual roots, the method has been used for observing hydrologic processes related to roots in 2-D or 3-D over time. Robinson *et al.* [2012] used time-lapse 3-D ERT to show that hydraulic redistribution in a pine forest from deep groundwater to the rooting zone was related to transport through tree roots. Additionally, Jayawickreme *et al.* [2008, 2010] collected time-lapse 2-D ERT data across a sharp ecotone in Michigan to estimate variations in soil moisture throughout the growing season for two plant communities: a deciduous forest and neighboring grassland. They found a significant difference between soil moisture before the start of the growing season (May) and in the peak of the growing season (August) under these two plant communities and a significantly larger seasonal change in soil moisture for the forest. They determined that trees have deeper effective roots, a finding that has substantial implications for alterations to hydrology due to changes in land cover. Similar to other time-lapse monitoring of hydrological processes with geophysics, the approach is usually limited to extraction of qualitative hydrological information rather than direct estimates of soil moisture change. Therefore, direct quantification of soil moisture uptake or changes in soil matric potential related to root zone processes is not easy to reliably obtain.

3.7.2. Gas Distribution and Movement in the Subsurface

Soil gas flux to the atmosphere and movement of gas within the subsurface are recognized as important to CZ processes [Lin, 2010]. In many cases, gas in the subsurface is a challenging geophysical target due to the complexity of an open system that is constantly mixing with ambient air. In general, parsing gas generated in situ apart from the atmospheric gas infiltrating at the ground surface is not currently possible using geophysics. Wetlands are an example of a special case in the CZ where the water table is close to surface and carbon-rich gas in the subsurface can be safely assumed to be generated in situ by subsurface biological processes and not mixed with the atmosphere. To date, most geophysical applications studying subsurface gas dynamics have been related to peat wetlands.

The adoption of noninvasive geophysical methods has permitted in situ measurements of CH₄ gas dynamics without having to insert direct gas content sensors through holes in a peatland, which disrupts the natural gas regime as evident from bubbling out of CH₄ observed from such activities. This highlights a major advantage of the geophysical approach as earlier studies of gas dynamics in peatlands inevitably required insertion of sensors and subsequent artificial gas releases [Waddington *et al.*, 2009]. Large changes in bulk physical properties accompany the production, transport, and release of gas in peatlands. Consequently, GPR has proven effective for locating hot spots of gas production and storage using physically based transforms to exploit the contrast in dielectric permittivity between gas and water [Parsekian *et al.*, 2011] and for monitoring releases of gas to the atmosphere in response to changes in buoyancy forces driven by atmospheric pressure and temperature variation [Comas *et al.*, 2008]. The remarkably high porosity of peat soils (typically > 0.9) means that multiphase volumetric mixing models, such as the complex refractive index

model, are relatively reliable (compared to typical mineral soils) for estimating gas content as uncertainty due to variations in the solid phase (peat fabric) is less important due to the small volume of the bulk material occupied by the solid phase. Evidence of gas redistribution/movement processes through trapping of gas beneath confining layers of more competent peat (partly due to the presence of wood layers) was identified at two peatlands [Comas *et al.*, 2013]—Sturgeon River 9 (Minnesota, USA) (Figure 7a) and Caribou Bog (Maine, USA) (Figure 7b). In contrast, a third peatland (Cors Fochno, Wales, UK) shows a homogenous distribution of free-phase gas (FPG) consistent with an absence of confining layers in this peatland. Seasonal GPR monitoring captures the accumulation of high concentrations of FPG in winter months, when the frozen peat surface acts as a confining layer preventing buoyancy-driven gas release, followed by abrupt release on thawing in the spring (Figure 7c) [Comas *et al.*, 2008]. Such information would be very challenging to acquire without a noninvasive geophysical method due to breaching of the trapped gas pockets with a direct sampler. Although currently specific to peatlands, these studies highlight a major advantage of geophysical methods to provide quantitative information on gas content, and even gas fluxes [Comas *et al.*, 2011], in an environment where traditional invasive methods can dramatically alter the natural subsurface gas regime and therefore provide erroneous information. Beyond detecting carbon-rich gas, recent research has demonstrated that geophysical measurements can contribute to assessment of carbon stocks in the critical zone, an important parameter in understanding carbon cycling through terrestrial systems [e.g., Lowry *et al.*, 2009; Parry *et al.*, 2014].

4. Discussion

4.1. Geophysical Measurement Strengths in CZ Research

Three main categories emerge where geophysical measurements of the CZ are advantageous: (1) to image distributions of subsurface properties in the space between direct measurements, (2) to acquire data on processes changing over time at the field scale, and (3) to reveal subsurface properties at large “exploration” scales of kilometers or more beyond what direct measurement can reveal.

With regards to the first category—imaging between direct measurements—geostatistical methods have proven effective for interpolating the subsurface structure between point data (i.e., wells, core, and borings). Geophysical measurements that are sensitive to the subsurface structure between direct point measurements provide significant additional constraints that can be used along with point observations to reduce interpolation uncertainty. Measurements of depth of weathering [Befus *et al.*, 2011], hydrostratigraphy [e.g., Pugin *et al.*, 2009], and aquifer geometry [e.g., Abraham *et al.*, 2012] provide examples of geophysical measurements that complement direct measurements to improve interpretations of CZ processes at a range of scales, reducing the need for interpolation between direct measurement points.

Regarding the second category, in some cases direct measurements simply may not be able to acquire enough information on, or may even disrupt, the process of interest. Obvious examples include estimating subsurface gas movement [e.g., Comas *et al.*, 2007], monitoring preferential water flow [Kim *et al.*, 2010], monitoring hydraulic redistribution processes in the root zone of soil [Robinson *et al.*, 2012], and exploring hyporheic exchange processes [e.g., Ward *et al.*, 2012; Mwakanyamale *et al.*, 2013]. In these examples, spatiotemporal imaging was essential to understanding the process.

The final category addresses the need to acquire data over larger areas relevant to catchment-scale (or larger) questions. Like lidar has revolutionized the way that Earth surface properties can be mapped over large areas, we believe that AEM has the potential to transform our understanding of subsurface properties by providing densely sampled data over large areas that are otherwise inaccessible. We have provided a series of examples demonstrating the spatial scale in AEM surveys where lakes (≥ 1 km across) and rivers (hundreds of meters across) were imaged entirely within the same data set, for example, permafrost groundwater/surface water interaction connections to regional groundwater [Minsley *et al.*, 2012]. Ground-based geophysical observations in similar environments are typically limited to transects that extend hundreds of meters to a few kilometers in length and allow for investigation of local phenomena but do not have the broad view needed to characterize regional features that have length scales of several kilometers or more. Moreover, AEM surveys avoid the logistical challenges of accessing remote or inaccessible terrain that limit ground-based observations.

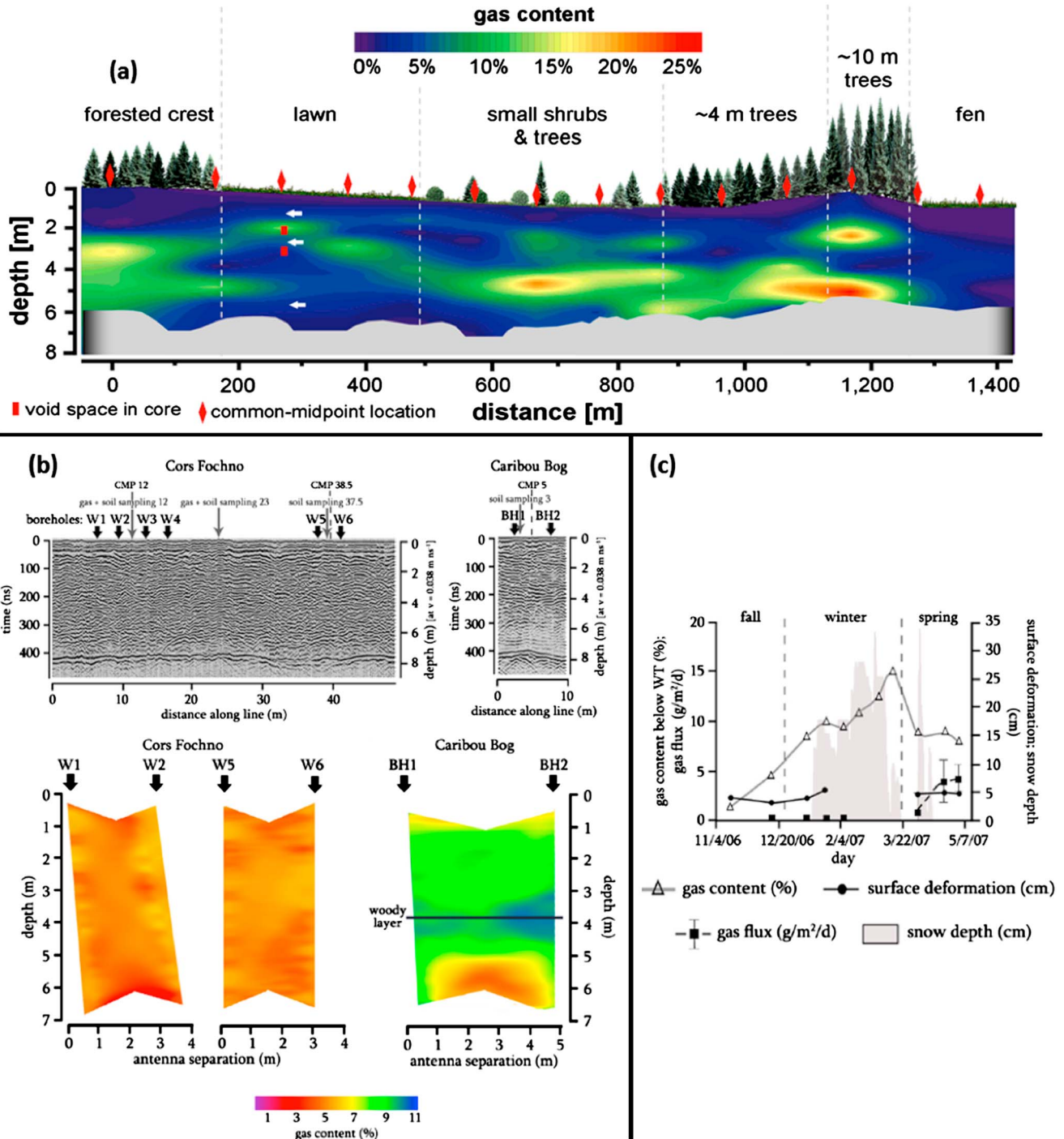


Figure 7. Examples of the use of ground-penetrating radar (GPR) to observe free-phase gas (FPG) in peatlands over multiple scales: (a) watershed-scale distribution of FPG across Sturgeon River (MN) obtained from 13 CMPs (red diamonds) showing interpolated distribution of FPG and evidence for storage below confining layers; (b) comparison of two bogs (Caribou Bog, ME, USA and Cors Fochno, Wales, UK) showing constant offset profiles (top) and estimated FPG distribution from cross-borehole GPR tomography. Caribou Bog again shows FPG trapped by competent peat fabric, whereas Cors Fochno shows a uniform distribution of FPG; (c) repeated GPR measurements of average FPG for 6 m peat column at Caribou Bog showing gas build up through the winter and subsequent release in the spring. Snow depth, surface deformation, and surface gas flux estimates are also shown. Figure 7a is after Parsekian et al. [2011], Figure 7b from Comas et al. [2013], and Figure 7c from Comas et al. [2008].

4.2. Contributions of Geophysics to Critical Zone Science

Numerous examples exist that demonstrate why geophysical measurements are a necessary and cost-effective way to constrain the boundary conditions that control CZ processes over different spatial scales and over the full depth range of the CZ. The principal purpose of multiscale geophysical imaging in the CZ is to gain new information about CZ processes that would not have been possible with other measurement methods alone.

Due to geophysical measurements, we now know that lithological boundaries (bedrock geology, weathering fronts) and mechanical processes such as fracturing set the stage for CZ structure and thus exert primary controls on CZ evolution [e.g., *Clarke and Burbank, 2011; Befus et al., 2011*]. These processes and controls cannot be adequately characterized, let alone understood, through studies that occur solely at the surface, in soil pits, and in widely spaced boreholes. Geophysical investigations of the weathering zone and processes that transform bedrock into regolith have revealed that saprolite has a much higher water-carrying capacity than previously thought and is likely a critical supporter of ecosystems in semiarid climates [*Holbrook et al., 2014*].

Geophysical imaging of hydrologic processes has also led to new understanding in CZ science. We reinforce this point by summarizing and highlighting several key examples. In the context of preferential flow, geophysical imaging has been used to show that dynamic hydrologic behavior exists within conduits in karst terrain [*Bumpus and Kruse, 2014*] and that hillslope drainage patterns can be explained by preferential flow through soil pipes in some systems [*Leslie and Heinse, 2013*]. Exchange between groundwater and surface water is relevant to a variety of other CZ processes, and geophysical imaging has revealed, for example, that the extent of the hyporheic zone changes with the seasons [*Ward et al., 2012*] and that heterogeneity of substream sediments [*Cardenas et al., 2004; Salehin et al., 2004*] and the presence of paleochannels [*Mwakanyamale et al., 2013*] control groundwater-surface water exchange. On regional scales, it is now known that in the discontinuous permafrost CZ of Alaska, thaw occurs below many lakes [*Minsley et al., 2012*], providing a hydraulic pathway that can connect lakes and rivers to deep groundwater [*Roach et al., 2011*]. However, *Jepsen et al.* [2013] also show that shallow flow in suprapermafrost aquifers can significantly control surface water budgets. Geophysical imaging of snow, particularly in the alpine CZ, has yielded new insights into the understanding of terrain controls on snowpack [*Marchand and Killingtveit, 2001*] as well as revealing the importance of snow to groundwater recharge.

The biological-terrestrial connection is fundamental in CZ science. Although noninvasive imaging of gas in the critical zone is challenging and is limited thus far to wetland critical zone environments, geophysical imaging has played a crucial role in revealing structural controls on subsurface biogenic gas movement in wetlands [*Comas et al., 2008, 2013*]. Time and spatially rich noninvasive imaging has also revealed biological drivers of hydrologic processes where deep water is redistributed within the rooting zone [*Robinson et al., 2012*].

4.3. Challenges for Geophysics in the CZ

Although there are a number of CZ scientific challenges that geophysical imaging is poised to address, one issue with many investigations is that geophysicists often explore systems at a resolution of the meter to submeter scale over only tens or hundreds of meters, which is too small for most watershed-scale problems, even though instrument deployments are possible on the larger scale. Airborne geophysical tools are well suited to address this considerable challenge of measuring properties at the right scales for catchment models. Mapping pathways at the watershed catchment scale has been achieved in numerous geological settings using airborne geophysical surveys [e.g., *Abraham et al., 2012*]. Understanding the geometry and interconnectedness of aquifer systems with sufficient spatial resolution over large areas is important for making accurate predictions about groundwater flow and transport.

Another primary challenge is overcoming the resistance to adoption of geophysical measurements. In some cases, CZ researchers that have relied on “traditional” measurements (borings, pits) of the subsurface are hesitant to adopt new technologies that may be viewed as untested. Furthermore, even if a geophysical measurement has been demonstrated to be robust for one application, there is not always evidence that it will be effective in another. To justify new applications and build confidence in the ability of geophysics to detect the parameters of interest, quantifiable “value of information” is required. Progress has been made in recent years at attempting to quantify the value of geophysical measurements for hydrologic science [e.g., *Nenna and Knight, 2013*], but the work has been limited.

A common disconnect between geophysical models and end users of these data is that images of geophysical property distributions do not directly address CZ science questions, for example, What is the depth of weathering? or What is the geometry of key confining layers or hydrologic pathways in the subsurface? It is important to frame the interpretation of geophysical data around the driving CZ question of interest. In some cases, providing constraints on the depth to a particular interface may be a more well-defined problem than the typical goal of mapping subtle or small-scale geophysical property heterogeneities.

Although geophysical technologies and underlying analysis tools are advancing rapidly, there are still limitations. Computing speed and power were previously limiting factors; however, these are now less significant issues with the advanced computing capability available today, even on desktop machines. Two key technical challenges for geophysical measurements that remain are the following: (1) understanding the physical property relationships that relate measured geophysical properties (e.g., electrical resistivity) to hydrogeologic properties of interest (e.g., lithology, salinity, and hydraulic conductivity) and (2) developing numerical strategies for integrating different types of data to improve models [Kowalsky *et al.*, 2005; Ferré *et al.*, 2009; Herckenrath *et al.*, 2013].

The former often places a firm constraint on how far the geophysicist can go with subsurface interpretation. Although theoretical and empirical relations between geophysical properties and hydraulic properties are extensively documented, they are inevitably of limited or minimal value when applied to large-scale geophysical images. The theoretical relations tend to be for simplified soils/rocks that do not represent the complexity of the pore-scale properties of natural soils/rocks in the subsurface. The empirical relations tend to be site specific and of uncertain predictive accuracy when applied outside of the range of materials used for the calibration. Consequently, geophysical information on the CZ is often restricted to definitions of boundaries (in the case of geological units) or volumes (in the case of movements of fluids), and the much needed next step to defining hydraulic properties from the geophysical data is quite correctly approached with much trepidation.

4.4. Opportunities for the Future

A relatively new methodology that can provide images of seismic V_s distribution in the subsurface is seismic interferometry or ambient noise correlation. This methodology has transformed approaches to crustal and mantle structure [e.g., Yang *et al.*, 2007; Bensen *et al.*, 2008]. The technique uses cross correlation of seismograms recorded at different receivers to retrieve the velocity structure (via a Green's function) between pairs of receivers; when data from a large number of receivers are included, 2-D and 3-D cross sections can be produced. The technique does not require active sources (e.g., from explosions or sledgehammer swings); assuming seismic energy propagating across a receiver array consists of isotropic plane waves sourced outside the array, images can be constructed solely from ambient noise. While recent work is pushing the technique to ever-shallower depths, most published studies of crustal inversions image over vertical scales of kilometers or tens of kilometers [Shapiro *et al.*, 2005]. A few studies, however, have begun applying the method to studies at depths and resolution relevant to the critical zone [Picozzi *et al.*, 2009; Pilz *et al.*, 2012, 2014]. Comparison of geological structure inferred from ambient noise tomography compares well at the 10 m lateral and vertical scale to coincident results from GPR and ERT transects [Picozzi *et al.*, 2009]. This technique shows much promise for producing 3-D images of subsurface structure in the critical zone.

Beyond enhanced applications of existing methods, there are opportunities in fields that currently see limited geophysical collaboration. For example, in ecohydrology, evaporation and transpiration are fundamental components of the terrestrial water balance and account for somewhere between half [Knight *et al.*, 1981; Trenberth *et al.*, 2007] to nearly all precipitation [Walvoord *et al.*, 2002] depending on climate. Some conceptual models note the interactions between the land-energy balance and groundwater depth [e.g., Maxwell *et al.*, 2007; Maxwell and Kollet, 2008] as shown by the three control regimes in Figure 8. This simulation indicates that very shallow groundwater does not exert control over latent heat flux nor does very deep groundwater. However, intermediate groundwater depths control latent heat flux in each of the projected climate scenarios. Consequently, mapping the depth to the water table, and soil moisture in the vadose zone, over large scales may be important to quantifying local water balances. Geophysical measurements such as ERT, seismic refraction, or GPR could potentially be used to interpolate water table depths between point measurements. Both GPR and ERT have been frequently used to image moisture content dynamics in the subsurface. This may be extended to the context of observing CZ system change in

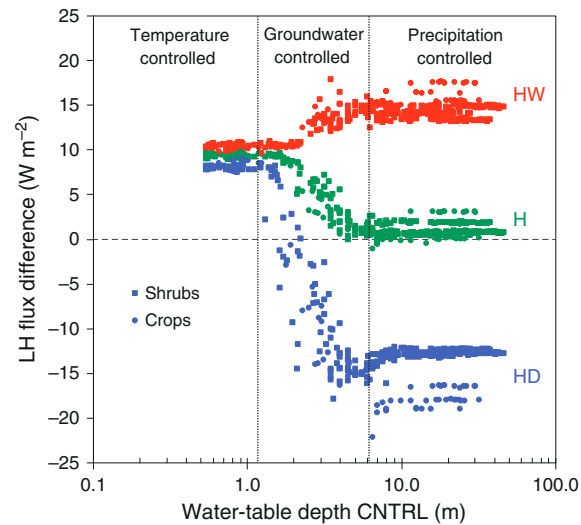


Figure 8. Plot of latent heat flux difference between the three perturbation cases (H = Hot; HW = Hot-Wet; and HD = Hot-Dry) and a control as a function of water table depth. Three regions: (1) a temperature-controlled region where latent heat flux is driven by atmospheric demand, (2) a groundwater-controlled region where latent heat flux is controlled by water table depth, and (3) a precipitation region where the water table is decoupled and latent heat flux is driven by rainfall are clearly shown in this figure (figure reprinted from Maxwell and Kollet [2008]).

response to future climate scenarios by measuring changes in subsurface conditions using long-term geophysical monitoring. For example, geophysical measurements of the regolith over time may reveal how weathering rates vary under a future warmer climate. Another example might be time-lapse geophysical investigation of variations in the products of biological activity (see section 3.7.2) due to climate forcing. This is particularly poignant because increased biological conversion of carbon to gases such as CO_2 or CH_4 may be a key positive feedback that could result in an increased rate of warming. We also see an opportunity for noninvasive biogeophysical imaging to be integrated more closely to CZ science. Limited studies exist using geophysics to image plant stems and tree trunks by capitalizing on the sensitivity to moisture; however, the processes observed are biological and not yet utilized in the framework of CZ science. For example, sapwood and hardwood have been imaged using ERT with electrodes in direct contact with the tree trunk to improve transpiration estimates [Bieker and Rust, 2010]. ERT has also been used to image tree rot [Bieker et al., 2010], and Jones et al. [2012] demonstrated the ability to track changes in moisture content of trees with NMR in 2-D. Long-term (months to years) self-potential monitoring has provided insight into the daily and seasonal timing and mechanisms of sap flow and other biophysical mechanisms associated with water uptake and tree function [Morat et al., 1994; Gibert et al., 2006]. In the future, these methods may be utilized in synoptic studies to gain a better understanding of how water and nutrients move through the CZ system as a whole. The geophysical signature of microbial biological activity is also being studied [Atekwana and Slater, 2009], however, largely in terms of contaminant remediation. We look forward to a future where these methods may be utilized to reveal naturally occurring microbiological processes in the CZ.

Magnetic geophysical methods are one of the most commonly used geophysical methods; however, these measurements are most often utilized in lithological mapping, and examples related to the observation of CZ processes are limited. In the geophysical sense, we most often think of magnetic methods being used to map the magnitude of the Earth's total field (or gradient) at some point or across an area. The magnetic susceptibility of a material may also be measured, although these measurements are usually made by logging a borehole or by analyzing hand samples. The relationship between magnetic susceptibility and historical weathering processes has been investigated [Bloemendal et al., 2008; Lu et al., 2008], and further research may reveal a connection between magnetic susceptibility and modern soil formation processes in the CZ. Changes in magnetic rock properties due to weathering under extreme conditions have been investigated [Chevrier et al., 2006]; however, similar to the previous examples, the measurements were made on extracted samples and not in the sense that we typically define field geophysical measurements as made at some distance from the target. An intriguing opportunity to observe a biological process in the CZ by its magnetic signature has been demonstrated in the context of hydrocarbon contamination remediation. Atekwana et al. [2014] show the microbial degradation of hydrocarbon by iron reducing bacteria results in a unique magnetic susceptibility signature. An investigation of the controls of magnetic susceptibility on soils showed that parent material and drainage are the primary controls while biological activity is observed to be a second-order effect [Blundell et al., 2009]. Nonetheless, we suggest that under the right conditions, a similar approach to Atekwana et al. [2014] could be used to monitor long-term natural biological activity in the CZ driven by natural forcing.

Another opportunity is the development of links between remote sensing and ground-based geophysics to study processes at scales larger than a catchment. There is a somewhat arbitrary and artificial divide between remote sensing methods (e.g., lidar, synthetic aperture radar, Landsat, and hyperspectral) acquired from satellite or airborne platforms and geophysical methods (e.g., electromagnetic, magnetics, and gravity) acquired from airborne or ground-based platforms. Both types of measurements are tools for indirectly measuring various physical properties of the Earth's near surface or subsurface. In addition, remote sensing and geophysical methods may be highly complementary to one another in terms of their sensitivity to physical properties, system processes, or spatial scales of interest, and although examples exist [e.g., *Pastick et al.*, 2013; *Liu et al.*, 2014], it is relatively infrequent to see these technologies combined in Earth science studies. Many satellite remote sensing methods rely on scattered electromagnetic energy of very short wavelength and are only sensitive to very shallow (< 1 m) features. On the other hand, airborne geophysical methods tend to have poor sensitivity to the very near surface but are capable of imaging properties to depths of up to several hundred meters. We agree with similar comprehensive assessments of geophysical methods [*Kruse*, 2013] that there is significant untapped potential in combining satellite—and airborne—platform remote sensing (either manned or drones) with ground-based geophysical measurements to link surface and subsurface observations.

5. Summary and Conclusions

Since the introduction of CZ studies, geophysical measurements have been recognized as key methods to measure parameters out of reach of direct measurement methods. We have highlighted examples of geophysical imaging methods that have been demonstrated to be effective for imaging parameters related to CZ processes on multiple scales, as well as examples of specific contributions to better understanding CZ science objectives that would not have been possible without geophysical imaging. Similarly, we have endeavored to suggest measurements that have a high likelihood for success that are not currently widely deployed. In many cases, geophysical measurements provide high spatial density, temporal richness, and noninvasive detection that traditional direct measurements may not be able to offer. Model accuracy is often limited by the scarcity of observations used for calibration. Combining feature-rich, yet indirect, geophysical observations with other traditional data has the potential to significantly improve model accuracy. We also identified opportunities, knowledge gaps, and new directions where geophysical measurements may support CZ science such as imaging of trees and linking remote sensing measurements with ground-based geophysics. We observe that for some applications, geophysical methods have been widely accepted, while in other cases adoption has been slower even though the technology is present and proven. Key points to reiterate are that (1) good geophysical targets have strong contrasts in physical properties, (2) water content and fluid chemistry often drive a contrast in geophysical properties, and therefore, hydrologic CZ processes are often most easily resolved in a time-lapse sense, (3) a key strength of geophysical measurements is spatially rich data sets that can be collected over time, and (4) a key weakness is that it is challenging at best to reliably convert geophysical properties to the physical properties the control CZ processes, particularly at the larger investigation scales.

We conclude that measurements of the critical zone using geophysical methods have acquired information about a range of parameters that would not have been possible using direct measurements, therefore enabling specific advances in CZ science. We found that observations related to weathering and hydrological processes were most prevalent, although emerging biogeophysical and ecological applications have a solid basis of work and a bright future.

Glossary

Airborne electromagnetics (AEM): A geophysical method that uses low-frequency electromagnetic energy transmitted into the Earth from a helicopter or fixed-wing aircraft-deployed system. Measurements of secondary magnetic fields are sensitive to subsurface electrical resistivity structure and can be acquired rapidly over large areas.

Critical zone: Earth's near surface that extends from the top of the trees to the bottom of the groundwater. A constantly evolving boundary layer where rock, soil, water, air, and living organisms interact (adapted from criticalzone.org).

Denitrification: Reduction of nitrates or nitrites facilitated by microbes that may ultimately release molecular nitrogen to the atmosphere.

Dielectric permittivity: A physical property relevant to high-frequency electromagnetic measurements (e.g., GPR) with distinct values for different materials such as air, rock, or water.

Distributed temperature sensing (DTS): A geophysical method that measures reflected laser pulses from microscopic imperfections in buried fiber-optic cable to make in situ temperature measurements.

Ecosystem services: The collective contributions of ecosystems that benefit people and society.

Ecotone: The transitional region between two adjacent ecosystems.

Electrical resistivity: A physical property that quantifies the ability of a material to conduct electrical current. Sometimes used interchangeably with its inverse, electrical conductivity. Relevant to low-frequency electromagnetic measurements (e.g., ERT and AEM). Can also be used synonymously with “electrical resistivity tomography”, referring to the geophysical method.

Electrical resistivity tomography (ERT): A geophysical method that injects electrical current through grounded electrodes and measures the associated voltage difference between other electrode pairs to infer subsurface electrical resistivity distributions.

Geophone: A geophysical instrument placed in contact with the ground to record motion generated by seismic waves.

GRACE (Gravity Recovery and Climate Experiment): Twin satellites that measure global-scale changes in Earth’s gravity field.

Ground-penetrating radar (GPR): A geophysical method that transmits and records reflected high-frequency electromagnetic waves sensitive to the dielectric permittivity of Earth materials.

Hyporheic zone: The area beneath and alongside streams and banks where surface water and groundwater exchange occurs.

Induced polarization (IP): A geophysical method that injects electrical current through grounded electrodes and measures the associated voltage and phase shift between other electrode pairs to infer subsurface electrical resistivity distributions and also to characterize grain-fluid interface properties.

Inversion: The data analysis process of taking measured data, forward modeling that data given whatever geometric parameters were used during measurement and the known underlying physics, and comparing the modeled data with the measured data. If it is possible to attain a small difference between the measured and the modeled data given some constraints imposed by the user (i.e., knowledge of what is geologically plausible), then it is possible to assume that the forward model is approximately representative of the true subsurface.

Landsat: A series of satellite missions that represents the world’s longest continuously acquired collection of space-based moderate-resolution land remote sensing data.

Lidar (light detection and ranging): A remote sensing method that uses reflected laser light to produce high-resolution topographic information.

Slope aspect: The compass direction that a slope faces (i.e., north, south, east, and west).

Nuclear magnetic resonance (NMR): A geophysical method that uses electromagnetic fields to excite the state of hydrogen protons in water molecules and measures the signal from those protons as they return from their perturbed state in order to infer subsurface water content.

Permafrost: Ground that has a temperature below 0°C for at least two consecutive years.

Regolith: A layer of unconsolidated rocky material that covers solid rock.

Seismic refraction: A geophysical method that transmits seismic waves into the subsurface and measures the returned energy determined by how the waves change direction in response to changes in the seismic velocity of different materials.

Seismic reflection: A geophysical method that transmits seismic waves into the subsurface and measures the energy returned by the impedance contrast at interfaces with contrasting seismic velocity and/or density.

Seismic velocity: A physical property that describes the speed of seismic waves in a particular material. Can refer to compressional (*P*) waves or shear (*S*) waves.

Self potential (SP): A geophysical method that measures the naturally occurring electrical voltages that can be generated in response to subsurface fluid flow or electrochemical processes.

Snow water equivalent (SWE): A measure of the amount of water within snowpack.

Surface wave methods: A seismic geophysical method that measures boundary waves that propagate along the Earth's surface to detect changes in shear wave velocity.

Tomography: A mathematical imaging process that can be applied to many types of geophysical data to produce estimates of the spatial distribution of subsurface physical properties.

Acknowledgments

We would like to thank the Editor-in-Chief M. Moldwin, S. Kruse, and two anonymous reviewers for their thoughtful comments that have greatly improved the quality of our manuscript.

The Editor for this paper was Gregory Okin. He thanks Sarah Kruse and three anonymous reviewers for their review assistance on this manuscript.

References

- Abraham, J. D., J. C. Cannia, P. A. Bedrosian, M. R. Johnson, L. B. Ball, and S. S. Sibray (2012), Airborne electromagnetic mapping of the base of aquifer in areas of western Nebraska, U.S. Geological Survey Scientific Investigations Report 2011-5219, 38 pp.
- Anderson, R. S., S. P. Anderson, and G. E. Tucker (2013), Rock damage and regolith transport by frost: An example of climate modulation of the geomorphology of the critical zone, *Earth Surf. Process. Landf.*, *38*(3), 299–316, doi:10.1002/esp.3330.
- Aster, R., B. Borchers, and C. Thurber (2005), *Parameter Estimation and Inverse Problems*, Academic Press, New York.
- Atekwana, E. A., and L. D. Slater (2009), Biogeophysics: A new frontier in Earth science research, *Rev. Geophys.*, *47*, RG4004, doi:10.1029/2009RG000285.
- Atekwana, E. A., F. M. Mewafy, G. Abdel Aal, D. D. Werkema, A. Revil, and L. D. Slater (2014), High-resolution magnetic susceptibility measurements for investigating magnetic mineral formation during microbial mediated iron reduction, *J. Geophys. Res. Biogeosci.*, *119*, 80–94.
- Barton, C. V. M., and K. D. Montagu (2004), Detection of tree roots and determination of root diameters by ground penetrating radar under optimal conditions, *Tree Physiol.*, *24*(12), 1323–1331, doi:10.1093/treephys/24.12.1323.
- Befus, K. M., A. F. Sheehan, M. Leopold, S. P. Anderson, and R. S. Anderson (2011), Seismic constraints on critical zone architecture, Boulder Creek watershed, Front Range, Colorado, *Vadose Zone J.*, *10*(4), 1342, doi:10.2136/vzj2010.0108er.
- Bensen, G. D., M. H. Ritzwoller, and N. M. Shapiro (2008), Broadband ambient noise surface wave tomography across the United States, *J. Geophys. Res.*, *113*, B05306, doi:10.1029/2007JB005248.
- Bieker, D., and S. Rust (2010), Electric resistivity tomography shows radial variation of electrolytes in *Quercus Robur*, *Can. J. Forest Res.*, *40*, 189–1193.
- Bieker, D., R. Kehr, G. Weber, and S. Rust (2010), Non-destructive monitoring of early stages of white rot by *Trametes versicolor* in *Fraxinus excelsior*, *Ann. Forest Sci.*, *67*(2), 210–210, doi:10.1051/forest/2009103.
- Binley, A., and A. Kemna (2005), DC resistivity and induced polarization methods, in *Hydrogeophysics*, edited by Y. Rubin and S. S. Hubbard, pp. 129–156, Springer, Netherlands.
- Bloemendal, J., X. Liu, Y. Sun, and N. Li (2008), An assessment of magnetic and geochemical indicators of weathering and pedogenesis at two contrasting sites on the Chinese Loess plateau, *Palaeogeogr. Palaeoclimatol. Palaeoecol.*, *257*(1), 152–168.
- Blundell, A., J. A. Dearing, J. F. Boyle, and J. A. Hannam (2009), Controlling factors for the spatial variability of soil magnetic susceptibility across England and Wales, *Earth Sci. Rev.*, *95*(3), 158–188.
- Bradford, J. H., J. T. Harper, and J. Brown (2009), Complex dielectric permittivity measurements from ground-penetrating radar data to estimate snow liquid water content in the pendular regime, *Water Resour. Res.*, *45*, W08403, doi:10.1029/2008WR007341.
- Brantley, S. L., et al. (2006), Frontiers in exploration of the critical zone: Report of a workshop sponsored by the National Science Foundation (NSF), 30 pp., Newark, Dec., 24 – 26 Oct.
- Braun, J.-J., et al. (2009), Regolith mass balance inferred from combined mineralogical, geochemical and geophysical studies: Mule Hole gneissic watershed, South India, *Geochim. Cosmochim. Acta.*, *73*(4), 935–961.
- Brunke, M., and T. Gonser (1997), The ecological significance of exchange processes between rivers and groundwater, *Freshwater Biol.*, *37*(1), 1–33, doi:10.1046/j.1365-2427.1997.00143.x.
- Bumpus, P. B., and S. E. Kruse (2014), Self-potential monitoring for hydrologic investigations in urban covered-karst terrain, *Geophysics*, *79*(6), B231–B242, doi:10.1190/geo2013-0354.1.
- Burtin, A., N. Hovius, D. T. Milodowski, Y.-G. Chen, Y.-M. Wu, C.-W. Lin, H. Chen, R. Emberson, and P.-L. Leu (2013), Continuous catchment-scale monitoring of geomorphic processes with a 2-D seismological array, *J. Geophys. Res. Earth Surf.*, *118*, 1956–1974, doi:10.1002/jgrf.20137.
- Butnor, J. R., J. A. Doolittle, L. Kress, S. Cohen, and K. H. Johnson (2001), Use of ground-penetrating radar to study tree roots in the southeastern United States, *Tree Physiol.*, *21*(17), 1269–1278, doi:10.1093/treephys/21.17.1269.
- Cardenas, M. B., and M. S. Markowski (2011), Geoelectrical imaging of hyporheic exchange and mixing of river water and groundwater in a large regulated river, *Environ. Sci. Technol.*, *45*(4), 1407–1411, doi:10.1021/es103438a.
- Cardenas, M. B., J. L. Wilson, and V. A. Zlotnik (2004), Impact of heterogeneity, bed forms, and stream curvature on subchannel hyporheic exchange, *Water Resour. Res.*, *40*, W08307, doi:10.1029/2004WR003008.
- Cassiani, G., A. Godio, S. Stocco, A. Villa, R. Deiana, P. Frattini, and M. Rossi (2009), Monitoring the hydrologic behaviour of a mountain slope via time-lapse electrical resistivity tomography, *Near Surf. Geophys.*, *7*(5–6), 475–486.
- Casto, D. W., B. Luke, C. Calderón-Macias, and R. Kaufmann (2009), Interpreting surface-wave data for a site with shallow bedrock, *J. Environ. Eng. Geophys.*, *14*(3), 115–127, doi:10.2113/JEEG14.3.115.
- Catchings, R. D., M. J. Rymer, M. R. Goldman, R. R. Sickler, and C. J. Criley (2014), A method and example of seismically imaging near-surface fault zones in geologically complex areas using V-P, V-S, and their ratios, *Bull. Seismol. Soc. Am.*, *104*, 1989–2006, doi:10.1785/0120130294.
- Chevrier, V., P. E. Mathé, P. Rochette, and H. P. Gunnlaugsson (2006), Magnetic study of an Antarctic weathering profile on basal: Implications for recent weathering on Mars, *Earth Planet. Sci. Lett.*, *244*(3), 501–514.
- Clarke, B. A., and D. W. Burbank (2011), Quantifying bedrock-fracture patterns within the shallow subsurface: Implications for rock mass strength, bedrock landslides, and erodibility, *J. Geophys. Res.*, *116*, F04009, doi:10.1029/2011JF001987.

- Comas, X., L. Slater, and A. Reeve (2007), In situ monitoring of ebullition from a peatland using ground penetrating radar (GPR), *Geophys. Res. Lett.*, *34*, L06402, doi:10.1029/2006GL029014.
- Comas, X., L. Slater, and A. Reeve (2008), Seasonal geophysical monitoring of biogenic gases in a northern peatland: Implications for temporal and spatial variability in free phase gas production rates, *J. Geophys. Res.*, *113*, G01012, doi:10.1029/2007JG000575.
- Comas, X., L. Slater, and A. S. Reeve (2011), Atmospheric pressure drives changes in the vertical distribution of biogenic free-phase gas in a northern peatland, *J. Geophys. Res.*, *116*, G04014, doi:10.1029/2011JG001701.
- Comas, X., N. Kettridge, A. Binley, L. Slater, A. Parsekian, A. J. Baird, M. Strack, and J. M. Waddington (2013), The effect of peat structure on the spatial distribution of biogenic gases within bogs, *Hydrol. Process.*, doi:10.1002/hyp.10056.
- Coscia, I., S. A. Greenhalgh, N. Linde, J. Doetsch, L. Marescot, T. Günther, T. Vogt, and A. G. Green (2011), 3D crosshole ERT for aquifer characterization and monitoring of infiltrating river water, *Geophysics*, *76*(2), G49–G59, doi:10.1190/1.3553003.
- Day-Lewis, F. D., K. Singha, and A. M. Binley (2005), Applying petrophysical models to radar travel time and electrical resistivity tomograms: Resolution-dependent limitations, *J. Geophys. Res.*, *110*, B08206, doi:10.1029/2004JB003569.
- Doetsch, J., N. Linde, C. Ilaria, G. Stewart, and A. Green (2010), Zonation for 3D aquifer characterization based on joint inversions of multi-method crosshole geophysical data, *Geophysics*, *75*, G53–G64, doi:10.1190/1.3496476.
- Ferré, T., L. Bentley, A. Binley, N. Linde, A. Kemna, K. Singha, K. Holliger, J. A. Huisman, and B. Minsley (2009), Critical steps for the continuing advancement of hydrogeophysics, *Eos*, *90*(23), 200–202.
- Fitterman, D. V., and M. Deszcz-Pan (1998), Helicopter EM mapping of saltwater intrusion in Everglades National Park, Florida, *Explor. Geophys.*, *29*, 240–243, doi:10.1071/EG998240.
- Fletcher, R. C., and S. L. Brantley (2010), Reduction of bedrock blocks as corestones in the weathering profile: Observations and model, *Am. J. Sci.*, *310*(3), 131–164, doi:10.2475/03.2010.01.
- Gibert, D., J.-L. Le Mouél, L. Lambs, F. Nicollin, and F. Perrier (2006), Sap flow and daily electric potential variations in a tree trunk, *Plant Sci.*, *171*, 572–584, doi:10.1016/j.plantsci.2006.06.012.
- Grasmueck, M. (1996), 3-D ground-penetrating radar applied to fracture imaging in gneiss, *Geophysics*, *61*(4), 1050–1064.
- Grauch, V. J. S., J. D. Phillips, D. J. Koning, P. S. Johnson, and V. Bankey (2009), Geophysical interpretations of the southern Espanola Basin, New Mexico, that contribute to understanding its hydrogeologic framework, U.S. Geological Survey Professional Paper 1761, 88 pp.
- Grelle, G., and F. M. Guadagno (2009), Seismic refraction methodology for groundwater level determination: “Water seismic index”, *J. Appl. Geophys.*, *68*, 301, doi:10.1016/j.jappgeo.2009.02.001.
- Hammond, G. E., and P. C. Lichtner (2010), Field-scale model for the natural attenuation of uranium at the Hanford 300 Area using high-performance computing, *Water Resour. Res.*, *46*, W09527, doi:10.1029/2009WR008819.
- Hansen, B. P., and J. W. Lane (1995), Use of surface and borehole geophysical surveys to determine fracture orientation and other site characteristics in crystalline bedrock terrain, Millville and Uxbridge, Massachusetts, US Department of the Interior, US Geological Survey.
- Herckenrath, D., G. Fiandaca, E. Auken, and P. Bauer-Gottwein (2013), Sequential and joint hydrogeophysical inversion using a field-scale groundwater model with ERT and TDEM data, *Hydrol. Earth Syst. Sci.*, *17*(10), 4043–4060, doi:10.5194/hess-17-4043-2013.
- Hertrich, M. (2008), Imaging of groundwater with nuclear magnetic resonance, *Prog. Nucl. Magn. Reson. Spectrosc.*, *53*(4), 227–248, doi:10.1016/j.pnmrs.2008.01.002.
- Hirano, Y., M. Dannoura, K. Aono, T. Igarashi, M. Ishii, K. Yamase, N. Makita, and Y. Kanazawa (2008), Limiting factors in the detection of tree roots using ground-penetrating radar, *Plant and Soil*, *319*, 15–24, doi:10.1007/s11104-008-9845-4.
- Holbrook, W. S., C. S. Riebe, M. Elwaseif, J. L. Hayes, K. Basler-Reeder, D. L. Harry, A. Malazian, A. Dosseto, P. C. Hartsough, and J. W. Hopmans (2014), Geophysical constraints on deep weathering and water storage potential in the Southern Sierra Critical Zone Observatory, *Earth Surf. Process. Landf.*, *39*(3), 366–380, doi:10.1002/esp.3502.
- Hsu, L., N. J. Finnegan, and E. E. Brodsky (2011), A seismic signature of river bedload transport during storm events, *Geophys. Res. Lett.*, *38*, L13407, doi:10.1029/2011GL047759.
- Irving, J., and R. Knight (2006), Numerical modeling of ground-penetrating radar in 2-D using MATLAB, *Comput. Geosci.*, *32*(9), 1247–1258.
- Irving, J., and K. Singha (2010), Stochastic inversion of tracer test and electrical geophysical data to estimate hydraulic conductivities, *Water Resour. Res.*, *46*, W11514, doi:10.1029/2009WR008340.
- Jackson, R. B., J. S. Sperry, and T. E. Dawson (2000), Root water uptake and transport: Using physiological processes in global predictions, *Trends Plant Sci.*, *5*, 482–488, doi:10.1016/S1360-1385(00)01766-0.
- Jaedicke, C. (2003), Snow mass quantification and avalanche victim search by ground penetrating radar, *Surv. Geophys.*, *24*(5–6), 431–445, doi:10.1023/B:GEOP.0000006075.80413.69.
- Jayawickreme, D., R. Van Dam, and D. Hyndman (2010), Hydrological consequences of land-cover change: Quantifying the influence of plants on soil moisture with time-lapse electrical resistivity, *Geophysics*, *75*(4), WA43–WA50, doi:10.1190/1.3464760.
- Jayawickreme, D. H., R. L. Van Dam, and D. W. Hyndman (2008), Subsurface imaging of vegetation, climate, and root-zone moisture interactions, *Geophys. Res. Lett.*, *35*, L18404, doi:10.1029/2008GL034690.
- Jepsen, S. M., C. I. Voss, M. A. Walvoord, B. J. Minsley, and J. Rover (2013), Linkages between lake shrinkage/expansion and sublacustrine permafrost distribution determined from remote sensing of interior Alaska, USA, *Geophys. Res. Lett.*, *40*, 882–887, doi:10.1002/grl.50187.
- Jin, L., and S. L. Brantley (2011), Soil chemistry and shale weathering on a hillslope influenced by convergent hydrologic flow regime at the Susquehanna/Shale Hills Critical Zone Observatory, *Appl. Geochem.*, *26*(Supplement), S51–S56, doi:10.1016/j.apgeochem.2011.03.027.
- Johnson, T. C., L. D. Slater, D. Ntargiannis, F. D. Day-Lewis, and M. Elwaseif (2012), Monitoring groundwater-surface water interaction using time-series and time-frequency analysis of transient three-dimensional electrical resistivity changes, *Water Resour. Res.*, *48*, W07506, doi:10.1029/2012WR011893.
- Jol, H. M. (Ed.) (2008), Ground penetrating radar theory and applications, Elsevier, Amsterdam.
- Jones, M., P. S. Aptaker, J. Cox, B. A. Gardiner, and P. J. McDonald (2012), A transportable magnetic resonance imaging system for in situ measurements of living trees: The Tree Hugger, *J. Magn. Reson.*, *218*, 133–140, doi:10.1016/j.jmr.2012.02.019.
- Jørgensen, F., et al. (2012), Transboundary geophysical mapping of geological elements and salinity distribution critical for the assessment of future sea water intrusion in response to sea level rise, *Hydrol. Earth Syst. Sci.*, *16*(7), 1845–1862, doi:10.5194/hess-16-1845-2012.
- Katul, G., P. Todd, D. Pataki, Z. J. Kabala, and R. Oren (1997), Soil water depletion by oak trees and the influence of root water uptake on the moisture content spatial statistics, *Water Resour. Res.*, *33*(4), 611–623, doi:10.1029/96WR03978.
- Keery, J., A. Binley, N. Crook, and J. W. N. Smith (2007), Temporal and spatial variability of groundwater-surface water fluxes: Development and application of an analytical method using temperature time series, *J. Hydrol.*, *336*(1–2), 1–16, doi:10.1016/j.jhydrol.2006.12.003.
- Kim, J. G., S.-G. Park, M.-J. Yi, and J.-H. Kim (2010), Tracing solute infiltration using a combined method of dye tracer test and electrical resistivity tomography in an undisturbed forest soil profile, *Hydrol. Process.*, *24*, 2977–2982.

- Knight, D. H., T. J. Fahey, S. W. Running, A. T. Harrison, and L. L. Wallace (1981), Transpiration from 100-yr-old lodgepole pine forests estimated with whole-tree potometers, *Ecology*, *62*(3), 717–726.
- Kowalsky, M. B., S. Finsterle, J. Peterson, S. Hubbard, Y. Rubin, E. Majer, A. Ward, and G. Gee (2005), Estimation of field-scale soil hydraulic and dielectric parameters through joint inversion of GPR and hydrological data, *Water Resour. Res.*, *41*, W11425, doi:10.1029/2005WR004237.
- Kruse, S. (2013), Near-surface geophysics in geomorphology, in *Treatise on Geomorphology, Remote Sensing and GIScience in Geomorphology*, vol. 3, edited by J. Shroder and M. P. Bishop, pp. 103–129, Academic Press, San Diego, Calif.
- Krause, S., D. M. Hannah, J. H. Fleckenstein, C. M. Heppell, D. Kaeser, R. Pickup, G. Pinay, A. L. Robertson, and P. J. Wood (2011), Inter-disciplinary perspectives on processes in the hyporheic zone, *Ecohydrology*, *4*(4), 481–499, doi:10.1002/eco.176.
- Leslie, I. N., and R. Heinse (2013), Characterizing soil-pipe networks with pseudo-three-dimensional resistivity tomography on forested hillslopes with restrictive horizons, *Vadose Zone J.*, *12*(4), doi:10.2136/vzj2012.0200.
- Lesmes, D. P., and S. P. Friedman (2005), Relationships between the electrical and hydrogeological properties of rocks and soils, in *Hydrogeophysics*, edited by Y. Rubin and S. S. Hubbard, pp. 87–128, Springer, Netherlands.
- Lin, H. (2010), Earth's critical zone and hydrogeology: Concepts, characteristics, and advances, *Hydrol. Earth Syst. Sci.*, *14*, 25–45, doi:10.5194/hess-14-25-2010.
- Liu, L., K. Schaefer, A. Gusmeroli, G. Grosse, B. M. Jones, T. Zhang, A. D. Parsekian, and H. A. Zebker (2014), Seasonal thaw settlement at drained thermokarst lake basins, Arctic Alaska, *Cryosphere*, *8*(3), 815–826, doi:10.5194/tc-8-815-2014.
- Loke, M. H., and R. D. Barker (1996), Rapid least-squares inversion of apparent resistivity pseudosections by a quasi-Newton method, *Geophys. Prospect.*, *44*, 131–152.
- Louie, J. N. (2001), Faster, better: Shear-wave velocity to 100 meters depth from refraction microtremor arrays, *Bull. Seismol. Soc. Am.*, *91*(2), 347–364, doi:10.1785/0120000098.
- Lowry, C. S., D. Fratta, and M. P. Anderson (2009), Ground penetrating radar and spring formation in a groundwater dominated peat wetland, *J. Hydrol.*, *373*(1–2), 68–79.
- Lu, S. G., Q. F. Xue, L. Zhu, and J. Y. Yu (2008), Mineral magnetic properties of a weathering sequence of soils derived from basalt in Eastern China, *Catena*, *73*(1), 23–33.
- Lundberg, A., C. Richardson-Näslund, and C. Andersson (2006), Snow density variations: Consequences for ground-penetrating radar, *Hydrol. Process.*, *20*(7), 1483–1495, doi:10.1002/hyp.5944.
- Marchand, W. D., and A. Killingtveit (2001), Analyses of the relation between spatial snow distribution and terrain characteristics, in *Proceedings of the 58th Eastern Snow Conference, Ottawa, Ontario, Canada: USA, Eastern Snow Conference*, edited by J. Hardy and S. Frankenstein, 71–84, Ottawa, Canada.
- Mavko, G., T. Mukerji, and J. Dvorkin (1998), *The Rock Physics Handbook: Tools for Seismic Analysis in Porous Media*, Cambridge Univ. Press, Cambridge, U. K.
- Maxwell, R. M., and S. J. Kollet (2008), Interdependence of groundwater dynamics and land-energy feedbacks under climate change, *Nat. Geosci.*, *1*(10), 665–669, doi:10.1038/ngeo315.
- Maxwell, R. M., F. K. Chow, and S. J. Kollet (2007), The groundwater–land–surface–atmosphere connection: Soil moisture effects on the atmospheric boundary layer in fully-coupled simulations, *Adv. Water Resour.*, *30*(12), 2447–2466, doi:10.1016/j.advwatres.2007.05.018.
- McClymont, A. F., J. W. Roy, M. Hayashi, L. R. Bentley, H. Maurer, and G. Langston (2011), Investigating groundwater flow paths within proglacial moraine using multiple geophysical methods, *J. Hydrology*, *399*(1), 57–69.
- McClymont, A. F., M. Hayashi, L. R. Bentley, and J. Liard (2012), Locating and characterizing groundwater storage areas within an alpine watershed using time-lapse gravity, GPR and seismic refraction methods, *Hydrol. Process.*, *26*(12), 1792–1804, doi:10.1002/hyp.9316.
- Meier, P., et al. (2014), Hydrogeophysical investigations in the western and north-central Okavango Delta (Botswana) based on helicopter and ground-based transient electromagnetic data and electrical resistance tomography, *Geophysics*, *79*(5), B201–B211.
- Menke, W. (1989), *Geophysical Data Analysis: Discrete Inverse Theory*, Academic Press, San Diego, Calif.
- Minsley, B. J., et al. (2012), Airborne electromagnetic imaging of discontinuous permafrost, *Geophys. Res. Lett.*, *39*, L02503, doi:10.1029/2011GL050079.
- Morat, P., J. L. Lemouel, and A. Granier (1994), Electrical potential on a tree: A measurement of the sap flow, *Compt. Rendus Acad. Des Sci. Serie III Sci. Vie*, *317*(1), 98–101.
- Moysey, S. M. J., and Z. Liu (2012), Can the onset of macropore flow be detected using electrical resistivity measurements?, *Soil Sci. Soc. Am. J.*, *76*(1), 10, doi:10.2136/sssaj2010.0413.
- Müller-Petke, M., and U. Yaramanci (2010), QT inversion—Comprehensive use of the complete SNMR dataset, *Geophysics*, *75*(4), WA199–WA209, doi:10.1190/1.3471523.
- Muskett, R. R., and V. E. Romanovsky (2009), Groundwater storage changes in arctic permafrost watersheds from GRACE and in situ measurements, *Environ. Res. Lett.*, *4*(4), 045009, doi:10.1088/1748-9326/4/4/045009.
- Mwakanyamale, K., F. D. Day-Lewis, and L. D. Slater (2013), Statistical analysis of zones of focused groundwater/surface-water exchange using fiber-optic distributed temperature sensing, *Water Resour. Res.*, *49*, 6979–6984, doi:10.1002/wrcr.20458.
- Nabighian, M. N., M. E. Ander, V. J. S. Grauch, R. O. Hansen, T. R. LaFehr, Y. Li, W. C. Pearson, J. W. Peirce, J. D. Phillips, and M. E. Ruder (2005), Historical development of the gravity method in exploration, *Geophysics*, *70*(6), doi:10.1190/1.2133785.
- Neal, A. (2004), Ground-penetrating radar and its use in sedimentology: Principles, problems and progress, *Earth Sci. Rev.*, *66*(3–4), 261–330, doi:10.1016/j.earscirev.2004.01.004.
- Nenna, V., and R. Knight (2013), Demonstration of a value of information metric to assess the use of geophysical data for a groundwater application, *Geophysics*, *79*(1), E51–E60.
- O'Connell, R. J., and B. Budiansky (1974), Seismic velocities in dry and saturated cracked solids, *J. Geophys. Res.*, *79*, 5412–5426, doi:10.1029/JB079i035p05412.
- Oldenborger, G. A., A. J.-M. Pugin, and S. E. Pullan (2013), Airborne time-domain electromagnetics, electrical resistivity and seismic reflection for regional three-dimensional mapping and characterization of the Spiritwood Valley Aquifer, Manitoba, Canada, *Near Surf. Geophys.*, *11*(1), 63–74, doi:10.3997/1873-0604.2012023.
- Oloná, J., J. A. Pulgar, G. Fernández-Viejo, C. López-Fernández, and J. M. González-Cortina (2010), Weathering variations in a granitic massif and related geotechnical properties through seismic and electrical resistivity methods, *Near Surf. Geophys.*, *8*(6), 585–599, doi:10.3997/1873-0604.2010043.
- Park, C., R. Miller, and J. Xia (1999), Multichannel analysis of surface waves, *Geophysics*, *64*(3), 800–808, doi:10.1190/1.1444590.
- Parker, E. H., Jr., and R. B. Hawman (2012), Multi-channel Analysis of Surface Waves (MASW) in Karst Terrain, Southwest Georgia: Implications for detecting anomalous features and fracture zones, *J. Environ. Eng. Geophys.*, *17*, 129–150.

- Parry, L. E., L. J. West, J. Holden, and P. J. Chapman (2014), Evaluating approaches for estimating peat depth, *J. Geophys. Res. Biogeosci.*, *119*, 567–576, doi:10.1002/2013JG002411.
- Parsekian, A. D., X. Comas, L. Slater, and P. H. Glaser (2011), Geophysical evidence for the lateral distribution of free phase gas at the peat basin scale in a large northern peatland, *J. Geophys. Res.*, *116*, G03008, doi:10.1029/2010JG001543.
- Pastick, N. J., M. T. Jorgenson, B. K. Wylie, B. J. Minsley, L. Ji, M. A. Walvoord, B. D. Smith, J. D. Abraham, and J. R. Rose (2013), Extending airborne electromagnetic surveys for regional active layer and permafrost mapping with remote sensing and ancillary data, Yukon Flats Ecoregion, Central Alaska, *Permafrost Periglac. Process.*, doi:10.1002/ppp.1775.
- Picozzi, M., S. Parolai, D. Bindi, and A. Strollo (2009), Characterization of shallow geology by high-frequency seismic noise tomography, *Geophys. J. Int.*, *176*, 164–174, doi:10.1111/j.1365-246X.2008.03966.x.
- Pilz, M., S. Parolai, M. Picozzi, and D. Bindi (2012), Three-dimensional shear wave velocity imaging by ambient seismic noise tomography, *Geophys. J. Int.*, *189*, 501–512, doi:10.1111/j.1365-246X.2011.05340.x.
- Pilz, M., S. Parolai, D. Bindi, A. Saponaro, and U. Abdybachaev (2014), Combining seismic noise techniques for landslide characterization, *Pure Appl. Geophys.*, *171*, 1729–1745, doi:10.1007/s00024-013-0733-3.
- Pollock, D., and O. A. Cirpka (2012), Fully coupled hydrogeophysical inversion of a laboratory salt tracer experiment monitored by electrical resistivity tomography, *Water Resour. Res.*, *48*, W01505, doi:10.1029/2011WR010779.
- Pride, S. (2005), Relationships between seismic and hydrological properties, in *Hydrogeophysics*, edited by Y. Rubin and S. Hubbard, pp. 253–291, Springer, Dordrecht, Netherlands.
- Pugin, A. J.-M., S. E. Pullan, J. A. Hunter, and G. A. Oldenborger (2009), Hydrogeological prospecting using P- And S-wave landstreamer seismic reflection methods, *Near Surf. Geophys.*, *7*(5–6), 315–327, doi:10.3997/1873-0604.2009033.
- Rabbel, W. (2010), Seismic methods, in *Groundwater Geophysics: A Tool for Hydrogeology*, edited by R. Kirsch, pp. 23–84, Springer, Berlin, doi:10.1007/978-3-540-88405-7.
- Refsgaard, J. C., et al. (2014), Nitrate reduction in geologically heterogeneous catchments—A framework for assessing the scale of predictive capability of hydrological models, *Sci. Total Environ.*, *468–469*, 1278–1288, doi:10.1016/j.scitotenv.2013.07.042.
- Rempe, D. M., and W. E. Dietrich (2014), A bottom-up control on fresh-bedrock topography under landscapes, *Proc. Natl. Acad. Sci. U.S.A.*, *111*(18), 6576–6581, doi:10.1073/pnas.1404763111.
- Revil, A., and A. Jardani (2013), *The Self-Potential Method*, Cambridge Univ. Press, Cambridge, U. K.
- Revil, A., L. Cary, Q. Fan, A. Finizola, and F. Trolard (2005), Self-potential signals associated with preferential ground water flow pathways in a buried paleo-channel, *Geophys. Res. Lett.*, *32*, L07401, doi:10.1029/2004GL022124.
- Rickenmann, D., J. M. Turowski, B. Fritschi, A. Klaiber, and A. Ludwig (2012), Bedload transport measurements at the Erlenbach stream with geophones and automated basket samplers, *Earth Surf. Process. Landf.*, *37*(9), 1000–1011, doi:10.1002/esp.3225.
- Rickenmann, D., et al. (2014), Bedload transport measurements with impact plate geophones: Comparison of sensor calibration in different gravel-bed streams, *Earth Surf. Process. Landf.*, *39*(7), 928–942, doi:10.1002/esp.3499.
- Roach, J., B. Griffith, B. Verbyla, and J. Jones (2011), Mechanisms influencing changes in lake area in Alaskan boreal forest, *Glob. Chang. Biol.*, *17*, 2567–2583, doi:10.1111/j.1365-2486.2011.02446.x.
- Robinson, J., T. Johnson, and L. Slater (2013), Evaluation of known-boundary and resistivity constraints for improving cross-borehole dc electrical resistivity imaging of discrete fractures, *Geophysics*, *78*(3), D115–D127, doi:10.1190/geo2012-0333.1.
- Robinson, J. L., L. D. Slater, and K. V. R. Schäfer (2012), Evidence for spatial variability in hydraulic redistribution within an oak-pine forest from resistivity imaging, *J. Hydrol.*, *430–431*, 69–79, doi:10.1016/j.jhydrol.2012.02.002.
- Rodell, M., J. Chen, H. Kato, J. Famiglietti, J. Nigro, and C. Wilson (2007), Estimating ground water storage changes in the Mississippi River basin (USA) using GRACE, *Hydrogeol. J.*, *15*(1), 159–166, doi:10.1007/s10040-006-0103-7.
- Running, S. W., and S. T. Gower (1991), Forest-BGC, a general-model of forest ecosystem processes for regional applications. II. Dynamic carbon allocation and nitrogen budgets, *Tree Physiol.*, *9*, 147–160.
- Sand, K., and O. Bruland (1998), Application of georadar in snow cover surveying, *Nord. Hydrol.*, *29*(4–5), 361–370.
- Salehin, M., A. I. Packman, and M. Paradis (2004), Hyporheic exchange with heterogeneous streambeds: Laboratory experiments and modeling, *Water Resour. Res.*, *40*, W11504, doi:10.1029/2003WR002567.
- Sassen, D. S., M. E. Everett, and C. L. Munster (2009), Ecohydrogeophysics at the Edwards aquifer: Insights from polarimetric ground-penetrating radar, *Near Surf. Geophys.*, *7*(5–6), 427–438.
- Scales, J. A., M. L. Smith, and S. Treitel (2001), *Introductory Geophysical Inverse Theory*, Samizdat Press, Golden, Colo.
- Schmandt, B., R. C. Aster, D. Scherler, V. C. Tsai, and K. Karlstrom (2013), Multiple fluvial processes detected by riverside seismic and infrasound monitoring of a controlled flood in the Grand Canyon, *Geophys. Res. Lett.*, *40*, 4858–4863, doi:10.1002/grl.50953.
- Seifert, D., T. O. Sonnenborg, P. Scharling, and K. Hinsby (2008), Use of alternative conceptual models to assess the impact of a buried valley on groundwater vulnerability, *Hydrogeol. J.*, *16*(4), 659–674, doi:10.1007/s10040-007-0252-3.
- Selker, J. S., L. Thévenaz, H. Huwald, A. Mallet, W. Luxemburg, N. van de Giesen, M. Stejskal, J. Zeman, M. Westhoff, and M. B. Parlange (2006), Distributed fiber-optic temperature sensing for hydrologic systems, *Water Resour. Res.*, *42*, W12202, doi:10.1029/2006WR005326.
- Shapiro, N. M., M. Campillo, L. Stehly, and M. H. Ritzwoller (2005), High-resolution surface-wave tomography from ambient seismic noise, *Science*, *307*, 1615–1618, doi:10.1126/science.1108339.
- Siemon, B., A. V. Christiansen, and E. Auken (2009), A review of helicopter-borne electromagnetic methods for groundwater exploration, *Near Surf. Geophys.*, *7*(5–6), 629–646, doi:10.3997/1873-0604.2009043.
- Slater, L. D., A. Binley, and D. Brown (1997), Electrical imaging of fractures using ground-water salinity change, *Groundwater*, *35*, 436–442, doi:10.1111/j.1745-6584.1997.tb00103.x.
- Slater, L. D., D. Ntarlagiannis, F. D. Day-Lewis, K. Mwakanyamale, R. J. Versteeg, A. Ward, C. Strickland, C. D. Johnson, and J. W. Lane Jr. (2010), Use of electrical imaging and distributed temperature sensing methods to characterize surface water–groundwater exchange regulating uranium transport at the Hanford 300 Area, Washington, *Water Resour. Res.*, *46*, W10533, doi:10.1029/2010WR009110.
- Slim, M., J. T. Perron, S. J. Martel, and K. Singha (2014), Topographic stress and rock fracture: A two dimensional numerical model for arbitrary topography and preliminary comparison with borehole observations, *Eart Surf. Process. Landf.*, doi:10.1002/esp.3646.
- Smith, B. D., J. D. Abraham, J. C. Cannia, B. J. Minsley, M. Deszcz-Pan, and L. B. Ball (2010), Helicopter electromagnetic and magnetic geophysical survey data, portions of the North Platte and South Platte Natural Resources Districts, western Nebraska, May 2009, U.S. Geol. Surv. Open File Rep. 1259: 33.
- Socco, L. V., and C. Strobbia (2004), Surface wave method for near-surface characterization: A tutorial, *Near Surf. Geophys.*, *2*, 165–185.
- Steeles, D. W. (2005), Shallow seismic methods, in *Hydrogeophysics*, edited by Y. Rubin and S. S. Hubbard, chap. 8, pp. 215–251, Springer, Netherlands.

- Sundström, N., D. Gustafsson, A. Kruglyak, and A. Lundberg (2013), Field evaluation of a new method for estimation of liquid water content and snow water equivalent of wet snowpacks with GPR, *Hydrol. Res.*, *44*(4), 600, doi:10.2166/nh.2012.182.
- Takagi, K., and H. S. Lin (2011), Temporal dynamics of soil moisture spatial variability in the Shale Hills Critical Zone Observatory, *Vadose Zone J.*, *10*(3), 832–842, doi:10.2136/vzj2010.0134.
- Tarantola, A. (2005), *Inverse Problem Theory and Methods for Model Parameter Estimation*, SIAM, Philadelphia, Pa.
- Tetzlaff, D., C. Birkel, J. Dick, J. Geris, and C. Soulsby (2014), Storage dynamics in hydrogeological units control hillslope connectivity, runoff generation, and the evolution of catchment transit time distributions, *Water Resour. Res.*, *50*, 969–985, doi:10.1002/2013WR014147.
- Toran, L., B. Hughes, J. Nyquist, and R. Ryan (2012), Using hydrogeophysics to monitor change in hyporheic flow around stream restoration structures, *Environ. Eng. Geosci.*, *18*(1), 83–97, doi:10.2113/gsegeosci.18.1.83.
- Trenberth, K. E., L. Smith, T. T. Qian, A. Dai, and J. Fasullo (2007), Estimates of the global water budget and its annual cycle using observational and model data, *J. Hydrometeorol.*, *8*(4), 758–769, doi:10.1175/JHM600.1.
- Truss, S., M. Grasmueck, S. Vega, and D. A. Viggiano (2007), Imaging rainfall drainage within the Miami oolitic limestone using high-resolution time-lapse ground-penetrating radar, *Water Resour. Res.*, *43*, W03405, doi:10.1029/2005WR004395.
- Tsoflias, G. P., J.-P. Van Gestel, P. L. Stoffa, D. D. Blankenship, and M. Sen (2004), Vertical fracture detection by exploiting the polarization properties of ground-penetrating radar signals, *Geophysics*, *69*(3), 803–810, doi:10.1190/1.1759466.
- Viezzoli, A., E. Auken, and T. Munday (2009), Spatially constrained inversion for quasi 3D modelling of airborne electromagnetic data—An application for environmental assessment in the Lower Murray Region of South Australia, *Explor. Geophys.*, *40*(2), 173–183, doi:10.1071/EG08027.
- Viezzoli, A., L. Tosi, P. Teatini, and S. Silvestri (2010), Surface water-groundwater exchange in transitional coastal environments by airborne electromagnetics: The Venice Lagoon example, *Geophys. Res. Lett.*, *37*, L01402, doi:10.1029/2009GL041572.
- Vrbancich, J., and P. K. Fullagar (2007), Towards remote sensing of sediment thickness and depth to bedrock in shallow seawater using airborne TEM, *Explor. Geophys.*, *38*(1), 77–88, doi:10.1071/EG07006.
- Waddington, J. M., S. J. Ketcheson, E. Kellner, M. Strack, and A. J. Baird (2009), Evidence that piezometers vent gas from peat soils and implications for pore-water pressure and hydraulic conductivity measurements, *Hydrol. Process.*, *23*, 1249–1254, doi:10.1002/hyp.7244.
- Walvoord, M. A., M. A. Plummer, F. M. Phillips, and A. V. Wolfsberg (2002), Deep arid system hydrodynamics: 1. Equilibrium state and response times in thick desert vadose zones, *Water Resour. Res.*, *38*(12), 1308, doi:10.1029/2001WR000824.
- Walvoord, M. A., C. I. Voss, and T. P. Wellman (2012), Influence of permafrost distribution on groundwater flow in the context of climate-driven permafrost thaw: Example from Yukon Flats Basin, Alaska, United States, *Water Resour. Res.*, *48*, W07524, doi:10.1029/2011WR011595.
- Wang, Y., S. A. Bradford, and J. Šimůnek (2013), Transport and fate of microorganisms in soils with preferential flow under different solution chemistry conditions, *Water Resour. Res.*, *49*, 2424–2436, doi:10.1002/wrcr.20174.
- Ward, A. S., M. N. Gooseff, and K. Singha (2010), Imaging hyporheic zone solute transport using electrical resistivity, *Hydrol. Process.*, *24*(7), 948–953, doi:10.1002/hyp.7672.
- Ward, A. S., M. Fitzgerald, M. N. Gooseff, T. J. Voltz, A. M. Binley, and K. Singha (2012), Hydrologic and geomorphic controls on hyporheic exchange during base flow recession in a headwater mountain stream, *Water Resour. Res.*, *48*, W04513, doi:10.1029/2011WR011461.
- Ward, S. H., and G. W. Hohmann (1988), Electromagnetic theory for geophysical applications, in *Electromagnetic Methods in Applied Geophysics: Volume 1. Theory*, edited by M. N. Nabighian, pp. 129–166, Society of Exploration Geophysicists, Tulsa, Okla.
- Wildenschild, D., K. H. Jensen, K. Villholth, and T. H. Illangasekare (1994), A laboratory analysis of the effect of macropores on solute transport, *Ground Water*, *32*(3), 381–389, doi:10.1111/j.1745-6584.1994.tb00655.x.
- Wishart, D. N., L. D. Slater, and A. E. Gates (2006), Self potential improves characterization of hydraulically-active fractures from azimuthal geoelectrical measurements, *Geophys. Res. Lett.*, *33*, L17314, doi:10.1029/2006GL027092.
- Wishart, D. N., L. D. Slater, and A. E. Gates (2008), Fracture anisotropy characterization in crystalline bedrock using field-scale azimuthal self potential gradient, *J. Hydrol.*, *358*(1–2), 35–45, doi:10.1016/j.jhydrol.2008.05.017.
- Worrall, L., T. J. Munday, and A. A. Green (1999), Airborne electromagnetics—Providing new perspectives on geomorphic process and landscape development in regolith-dominated terrains, *Phys. Chem. Earth Solid Earth Geodes.*, *24*(10), 855–860, doi:10.1016/S1464-1895(99)00127-1.
- Wroblicky, G. J., M. E. Campana, H. M. Valett, and C. N. Dahm (1998), Seasonal variation in surface-subsurface water exchange and lateral hyporheic area of two stream-aquifer systems, *Water Resour. Res.*, *34*(3), 317–328, doi:10.1029/97WR03285.
- Xia, J., R. D. Miller, and C. B. Park (1999), Estimation of near-surface shear-wave velocity by inversion of Rayleigh waves, *Geophysics*, *64*, 691–700.
- Yang, Y., M. H. Ritzwoller, A. L. Levshin, and N. M. Shapiro (2007), Ambient noise Rayleigh wave tomography across Europe, *Geophys. J. Int.*, *168*, 259–274, doi:10.1111/j.1365-246X.2006.03203.x.
- Yokota, Y., M. Matsumoto, A. Gaber, M. Grasmueck, and M. Sato (2011), Estimation of biomass of tree roots by GPR with high accuracy positioning system, in *Geoscience and Remote Sensing Symposium (IGARSS)*, 2011 IEEE International, pp. 190–193.
- Yoshikawa, K., and L. D. Hinzman (2003), Shrinking thermokarst ponds and groundwater dynamics in discontinuous permafrost near Council, Alaska, *Permafrost Periglac. Process.*, *14*(2), 151–160, doi:10.1002/ppp.451.
- Zenone, T., G. Morelli, M. Teobaldelli, F. Fischanger, M. Matteucci, M. Sordini, A. Armani, C. Ferrè, T. Chiti, and G. Seufert (2008), Preliminary use of ground-penetrating radar and electrical resistivity tomography to study tree roots in pine forests and poplar plantations, *Funct. Plant Biol.*, *35*(10), 1047–1058, doi:10.1071/FP08062.
- Zonge, K., J. Wynn, and S. Urquhart (2005), Resistivity, induced polarization and complex resistivity, in *Near-Surface Geophysics*, edited by D. K. Butler, pp. 265–300, Society of Exploration Geophysicists, Tulsa, Okla.